

การเตรียมอนุภาคโคโตซานด้วยอัลตราโซนิคอะตอมไมเซชัน
สำหรับการปลดปล่อยยาแบบควบคุม

นางสาววิลาวัณย์ ท่องกง

สถาบันวิทยบริการ
จุฬาลงกรณ์มหาวิทยาลัย

วิทยานิพนธ์นี้เป็นส่วนหนึ่งของการศึกษาตามหลักสูตรปริญญาวิทยาศาสตรมหาบัณฑิต

สาขาวิชาปิโตรเคมีและวิทยาศาสตร์พอลิเมอร์

คณะวิทยาศาสตร์ จุฬาลงกรณ์มหาวิทยาลัย

ปีการศึกษา 2550

ลิขสิทธิ์ของจุฬาลงกรณ์มหาวิทยาลัย

PREPARATION OF CHITOSAN PARTICLES USING ULTRASONIC
ATOMIZATION FOR CONTROLLED DRUG RELEASE

Miss Wilawan Thongkong

A Thesis Submitted in Partial Fulfillment of the Requirements
for the Degree of Master of Science Program in Petrochemistry and Polymer Science

Faculty of Science

Chulalongkorn University

Academic Year 2007

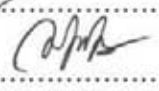
Copyright of Chulalongkorn University

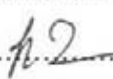
วิลาวัณย์ ท่องคง: การเตรียมอนุภาคไคโตซานด้วยอัลตราโซนิคอะตอมไมเซชันสำหรับการปลดปล่อยยาแบบควบคุม (PREPARATION OF CHITOSAN PARTICLES USING ULTRASONIC ATOMIZATION FOR CONTROLLED DRUG RELEASE) อ. ที่ปรึกษา: ผศ. ดร.วราวุฒิ ตั้งพสุธาตล, อ. ที่ปรึกษาร่วม: ดร.กฤษณา ศิริเลิศมุกด, 85 หน้า.

ได้เตรียมอนุภาคไคโตซานที่มีขนาด 250 ถึง 1,520 นาโนเมตรจากสารละลายไคโตซานโดยใช้เครื่องอเล็กโตรสเปรย์ที่ติดตั้งอัลตราโซนิคอะตอมไมเซอร์ไว้ อนุภาคที่ได้เป็นทรงกลมที่มีผิวเรียบ เมื่อศึกษาผลของตัวแปรการเตรียมต่างๆ ต่อขนาดอนุภาคพบว่าเมื่อน้ำหนักโมเลกุลเพิ่มขึ้นจาก 47 ถึง 238 kDa ขนาดของอนุภาคแห้งมีแนวโน้มเพิ่มขึ้นแต่ไม่มีนัยสำคัญ แต่ในสภาวะเปียกนั้นขนาดอนุภาคกลับเพิ่มขึ้นอย่างมีนัยสำคัญ เมื่อต้องการอนุภาคไคโตซานขนาดเล็ก ไคโตซานที่ใช้ควรมีค่า DD สูง และสารละลายความเข้มข้นต่ำ การเพิ่มปริมาณยาลิโคเคนมีแนวโน้มทำให้ขนาดอนุภาคแห้งใหญ่ขึ้นอย่างมีนัยสำคัญแต่ไม่มีนัยสำคัญสำหรับอนุภาคเปียก ผลการวิเคราะห์อนุภาคไคโตซานที่มีลิโคเคนด้วยไออาร์พบการเพิ่มขึ้นของพันธะไฮโดรเจนระหว่างไคโตซานและลิโคเคน ปริมาณลิโคเคนภายในอนุภาค CS-LC-Ps เพิ่มขึ้นเมื่อเพิ่มสัดส่วนระหว่างยาและไคโตซาน แต่จะลดลงเมื่อใช้ไคโตซานที่มีน้ำหนักโมเลกุลเพิ่มขึ้น ค่าประสิทธิภาพการกักเก็บนั้นสามารถเตรียมได้ถึง 90% จากผลการศึกษาการปลดปล่อยยาพบว่าลิโคเคนปริมาณสูงถึง 92% ปลดปล่อยออกมาจากอนุภาคไคโตซานในฟอสเฟตบัฟเฟอร์ (พีเอช 7.4) ที่อุณหภูมิ 37°C ได้ภายในเวลา 3 ชั่วโมงโดยไม่มีภาวะระเบิดออกของปริมาณยาในช่วงแรกของการแช่ในสารละลาย สุดท้ายเป็นการศึกษาเลียนแบบสภาวะการซึมผ่านผิวหนังของลิโคเคนจากอนุภาคไคโตซานโดยใช้คราบงูและเมมเบรนเซลลูโลส พบว่ามีลิโคเคนปลดปล่อยออกมาอย่างต่อเนื่องตลอดระยะเวลาที่ศึกษานาน 6 ชั่วโมง

สาขาวิชา ปีโตรเคมีและวิทยาศาสตร์พอลิเมอร์ ลายมือชื่อนิสิต..... 

ปีการศึกษา 2550

ลายมือชื่ออาจารย์ที่ปรึกษา..... 

ลายมือชื่ออาจารย์ที่ปรึกษาร่วม..... 

4872469423: MAJOR PETROCHEMISTRY AND POLYMER SCIENCE

KEY WORD: CHITOSAN/PARTICLES/ULTRASONIC ATOMIZATION/
DRUG RELEASE

WILAWAN THONGKONG: PREPARATION OF CHITOSAN PARTICLES USING ULTRASONIC ATOMIZATION FOR CONTROLLED DRUG RELEASE. THESIS ADVISOR: ASST. PROF. VARAWUT TANGPASUTHADOL, PhD, THESIS CO-ADVISOR: KRISANA SIRALEARTMUKUL, PhD, 85 pp.

Chitosan particles with the sizes ranging from 250 to 1,520 nm was prepared from chitosan solution using an electrospray equipped with an ultrasonic atomizer. The chitosan particles were spherical and had smooth surface. The effects of preparation parameters on particle size were investigated. The size of dry chitosan particles tended to increase but not statistically significant when the molecular weights increased from 47 to 238 kDa. But in the hydrated state the particle sizes increased significantly with increasing the MW. In order to get small CS particle size, CS with high DD and low CS concentration should be used. Increasing the lidocaine drug content tended to significantly increase the size of dry particles but not the hydrated particles. Increasing in hydrogen bonding between chitosan and lidocaine was observed by IR analysis. The lidocaine content within CS-LC-Ps was increased with the increasing drug to chitosan ratio but decreased with chitosan molecular weight increased. The entrapment efficiency of 90% could be successfully achieved. Up to 92% of lidocaine was released from chitosan particles into phosphate buffer solution (pH 7.4) at 37°C within the period of 3 hours with no significant burst of drug during the initial hydrated stage. Finally, a simulated skin permeation study of the lidocaine from chitosan particles using shed snake skin and cellulose membrane demonstrated that lidocaine was continuously released from the particles for up to 6 hours of study.

Field of Study Petrochemistry and Polymer Science

Academic Year 2007

Student's Signature.....

Advisor's Signature.....

Co-advisor's Signature.....

ACKNOWLEDGEMENTS

The author thanks many people for kindly providing the knowledge of this study. First, I would like to express gratitude and appreciation to my advisor, Assistant Professor Dr. Varawut Tangpasuthadol and co-advisor, Dr. Krisana Siralermukul for invaluable guidance and suggestions throughout this work.

I express my warmest gratitude to Suwalee Chandrkrachang, for sharing her long experience in the field of chitosan and for her suggestions and advice. I am especially thankful to Sira Pochana and Pol Polsan, EBASE Corporation, for kindly supporting the Nano particle reactor used in this work.

I wish to express my grateful thank to Associate Professor Dr. Supawan Tantayanon, chairman of thesis committee for her valuable advice. I also express my appreciation to Assistant Professor Dr. Voravee P. Hoven and Dr. Pranee Lertsutthiwong, thesis committee members for their invaluable comments suggestions. I would also like to thank the National Research Council of Thailand for financial support. My appreciation is extended to Queen Saovabha Memorial Institute for its kindly contribution of shed snake skin of *Naja kaouthia* used throughout this study.

Furthermore, the author also thank the Center of Chitin-Chitosan Biomaterial, Metallurgy and Materials Science Research Institute of Chulalongkorn University for providing the equipment, chemicals, and facilities. I thank the National Nanotechnology Center (NANOTEC) for facilitating the Zetasizer Nano ZS for particle size measurement.

Finally, I would like to express my honest thanks to my family especially my parents and sister for their help, cheerful, endless love, understanding and encouragement.

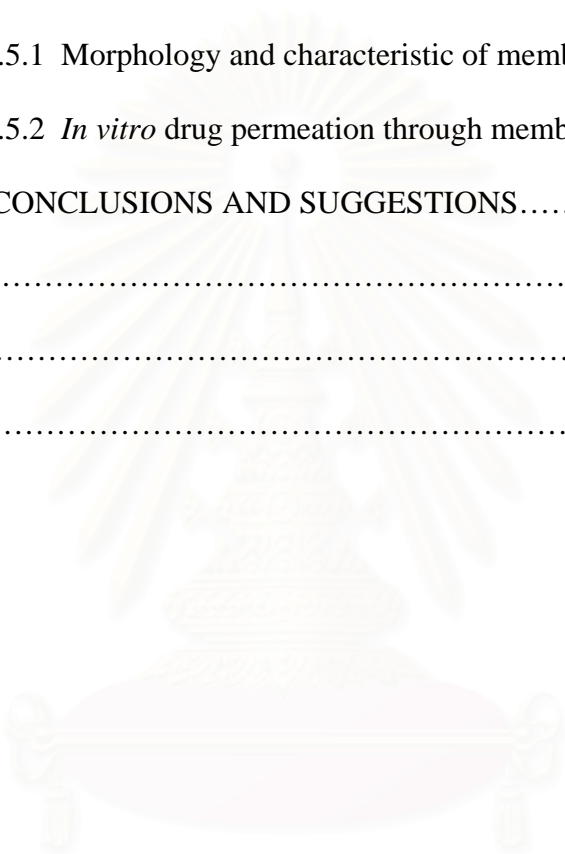
CONTENTS

	PAGE
ABSTRACT (IN THAI).....	iv
ABSTRACT (IN ENGLISH).....	v
ACKNOWLEDGEMENTS.....	vi
CONTENTS.....	vii
LIST OF TABLES	xi
LIST OF FIGURES	xiii
LIST OF ABBREVIATIONS.....	xvi
CHAPTER I INTRODUCTION.....	1
1.1 Rationale	1
1.2 Objectives	3
1.3 Scope and work.....	3
CHAPTER II THEORY AND LITERATURE REVIEW.....	4
2.1 Chitosan.....	4
2.2 Lidocaine.....	5
2.3 Particle generator.....	7
2.3.1 Nano particle reactor.....	7
2.3.2 Spray drying technique.....	8
2.4 Literature review on micro/nanoparticles preparation for controlled drug release.....	9
2.5 Controlled release system.....	13

	PAGE
2.6 Transdermal delivery systems.....	16
2.7 Franz' s cell apparatus.....	16
2.8 Skin sources.....	17
CHAPTER III EXPERIMENTAL.....	20
3.1 Materials.....	20
3.2 Characterization of chitosan samples.....	20
3.2.1 Molecular weight of chitosan.....	20
3.2.2 Solubility of chitosan.....	21
3.2.3 Degree of deacetylation.....	21
3.2.4 Apparent viscosity.....	22
3.3 Preparation of low molecular weight chitosan by ultrasonication.....	22
3.4 Particles preparation.....	23
3.5 Characterization of particles.....	24
3.5.1 Microscopic analysis.....	24
3.5.2 Particle size measurement.....	24
3.5.3 Functional group analysis.....	25
3.5.4 Powder x-ray diffraction study.....	25
3.6 Evaluation of drug content and drug entrapment efficiency.....	25
3.6.1 Calibration curve of lidocaine for UV spectroscopy.....	25
3.6.2 Determination of drug content.....	26
3.6.3 Determination of drug entrapment efficiency (EE).....	26

	PAGE
3.7 <i>In vitro</i> lidocaine release from chitosan nanoparticles	27
3.7.1 Preparation of buffer medium for drug release study.....	27
3.7.2 Calibration curve of lidocaine in buffer solution	27
3.7.3 <i>In vitro</i> drug release.....	27
3.8 <i>In vitro</i> study of drug permeation through shed snake skin and cellulose membrane.....	28
3.8.1 Drug permeation studies.....	28
3.8.2 Buffer medium preparation.....	30
3.8.3 Characteristic of shed snake skin.....	30
3.8.4 Characteristic of cellulose membrane.....	31
3.9 Statistical analysis.....	31
CHAPTER IV RESULTS AND DISCUSSION.....	32
4.1 Characterization of chitosan	32
4.2 Preparation of chitosan particles and lidocaine association.....	33
4.2.1 Comparison of particles morphology as produced from ultrasonic atomization and spray dry technique.....	34
4.2.2 Physical characterization of particles.....	35
4.2.3 Interaction between lidocaine and chitosan systems.....	40
4.2.4 Degree of crystallinity of lidocaine in matrix particles....	41
4.3 Evaluation of drug entrapment efficiency in chitosan particles.....	42

	PAGE
4.4 Drug release study of chitosan particles in phosphate buffer medium	44
4.5 <i>In vitro</i> study of lidocaine permeation through membrane.....	46
4.5.1 Morphology and characteristic of membranes	46
4.5.2 <i>In vitro</i> drug permeation through membranes	48
CHAPTER V CONCLUSIONS AND SUGGESTIONS.....	52
REFERENCES.....	54
APPENDICES.....	61
VITAE.....	85



 สถาบันวิทยบริการ
 จุฬาลงกรณ์มหาวิทยาลัย

LIST OF TABLES

TABLE	PAGE
2.1 The animal skins that have been used in permeation studies.....	18
3.1 The parameters studied for the particle preparation by using an ultrasonic atomization technique	24
4.1 General characteristics of chitosan (CS) used for particle preparation.....	32
4.2 Viscosity and molecular weight of chitosan upon changing the amplitude of ultrasonication at a fixed period of 1 h (chitosan concentration = 0.25%w/v, 75 kDa).....	33
4.3 Effect of molecular weight on particle size of CS-Ps.....	37
4.4 Effect of %DD on particle size of CS-Ps.....	38
4.5 Effect of chitosan concentration on particle size of CS-Ps.....	38
4.6 Effect of lidocaine to chitosan mass ratio on particle size of CS-LC-Ps...	39
4.7 Effect of chitosan molecular weight on particle size of CS-LC-Ps.....	39
4.8 Peak position and Assignment of CS-LC-Ps (A), LC (B) and CS-Ps (C).....	41
4.9 Lidocaine content and entrapment efficiency (%EE) at different lidocaine to chitosan mass ratios.....	43
4.10 Lidocaine content and entrapment efficiency (%EE) at different the chitosan molecular weight (condition: CS conc. = 0.5%CS).....	43
4.11 The thickness of shed snake skin and lipid within shed snake skin.....	48

TABLE	PAGE
4.12 Linear relationship between the amount of drug permeating through one area division of shed snake skin (Q_p) and time	50
4.13 Linear relationship between the amount of drug permeating through one area division of cellulose membrane (Q_p) and time	51



สถาบันวิทยบริการ
จุฬาลงกรณ์มหาวิทยาลัย

LIST OF FIGURES

FIGURE	PAGE
1.1 Chemical structure of chitin and chitosan	1
1.2 Schematic presentation of preparation of particles using ultrasonic atomization technique.....	2
2.1 Structures of chitin and chitosan	5
2.2 The structure of lidocaine hydrochloride.....	6
2.3 Presentation of Nano particle reactor equipped with an ultrasonic atomizer unit.....	8
2.4 Schematic representation of spray drying technique.....	9
2.5 Presentation of controlled release system.....	13
2.6 Presentation of diffusion controlled release.....	14
2.7 Presentation of swelling controlled release.....	15
2.8 Presentation of erosion controlled release.....	15
2.9 The components of Franz' s cell.....	17
3.1 Schematic presentation of ultrasonic probe.....	23
3.2 The components of Franz' s cell (a) and instrument set-up for permeation study (b).....	29
4.1 Scanning electron micrographs of chitosan particles prepared by ultrasonic atomization technique (a) and spray dry (b) produced from CS molecular weight of 75 kDa with 0.5% CS (w/v)....	34

FIGURE	PAGE
4.2 Scanning electron micrographs of blank CS-Ps (a, b), CS-LC-Ps (LC:CS = 0.5:1) (c), and CS-LC-Ps (LC:CS = 1:1) (d), produced from 0.5%CS solution (CS molecular weight = 75 kDa).....	35
4.3 Scanning electron micrographs of CS-LC-Ps (LC:CS = 0.33:1) (a), CS-LC-Ps (LC:CS = 0.5:1) (b), and CS-LC-Ps (LC:CS = 1:1) (c), produced from 0.25%CS solution (CS molecular weight = 47 kDa).....	36
4.4 FT-IR spectra of CS-LC-Ps (LC:CS = 1:1) (a), lidocaine hydrochloride (b), and CS-Ps (c).....	40
4.5 X-Ray diffractograms of CS-LC-Ps (LC:CS = 1:1) (a), lidocaine hydrochloride (b), and CS-Ps (c).....	42
4.6 Comparison of cumulative LC release of CS-LC-Ps having different chitosan to drug ratios (Mw of CS = 47 kDa; CS conc.= 0.25%CS). Error bars indicate the range of experimental reading obtained (sample number, $n = 3$).....	44
4.7 Comparison of %cumulative lidocaine release of CS-LC-Ps having different chitosan to drug ratios (Mw of CS=47 kDa; CS conc.= 0.25%CS). Error bars indicate the range of experimental reading obtained (sample number, $n = 3$).....	45
4.8 SEM of CS-LC-Ps (LC:CS mass ratio = 0.5:1) after incubation at 37°C for 6 h in phosphate buffer (pH = 7.4). The incubated particles either remained as particles with cracks (a) or disintegrate into fibrous matrix (b).....	46

FIGURE	PAGE
4.9 General characteristics of shed snake skin specimens from <i>Naja kaouthia</i>	46
4.10 SEM of dorsal scale of shed snake skin specimens from <i>Naja kaouthia</i> ; (a)×5,000 and (b)×10,000.....	47
4.11 SEM of dorsal hinge of shed snake skin specimens from <i>Naja kaouthia</i> ; (a)×5,000 and (b)×10,000.....	47
4.12 Permeation profiles of drug through shed snake skin (<i>Naja kaouthia</i>) at various lidocaine to chitosan mass ratios.	49
4.13 Permeation profiles of drug through cellulose membrane at various lidocaine to chitosan mass ratio.....	51

LIST OF ABBREVIATIONS

%	: percentage
µg	: microgram
APDs	: avalanche photodiode array
cm	: centimeter
conc.	: concentration
cps	: centipoises
CS	: chitosan
CS-LC-Ps	: chitosan-lidocaine particles
CS-Ps	: chitosan particles
DD	: degree of deacetylation
DLS	: data least squares
DNA	: deoxyribonucleic acid
EE	: entrapment efficiency
F	: flux
FTIR	: Fourier Transform Infrared Spectrophotometer
g	: gram
h	: hour
kDa	: kilodalton
LC	: lidocaine
LC:CS	: lidocaine:chitosan
M	: concentration in molar
mA	: milliamperes
mg	: milligram
min	: minute
mL	: milliliter
mW	: milliwatt
MW	: molecular weight
nm	: nanometer
PDI	: polydispersity index

pDNA	: plasmid deoxyribonucleic Acid
pH	: power of hydrogen ion or the negative logarithm (base ten)
Q_p	: Cumulative amount of drug permeated through a unit area of cellulose membrane/shed snake skin
rpm	: round per minute
SD	: standard deviation
SEM	: Scanning Electron Microscope
t	: time
UV	: ultraviolet
v/v	: volume/volume
w/w	: weight/weight
w/v	: weight/volume
XRD	: X-ray diffractrometer



สถาบันวิทยบริการ
จุฬาลงกรณ์มหาวิทยาลัย

CHAPTER I

INTRODUCTION

1.1 Rationale

Chitosan is a cationic polysaccharide derived from naturally occurring chitin in crab and shrimp shells by deacetylation process (Figure 1.1). Chitosan is reportedly a hydrophilic, nontoxic, biocompatible and biodegradable polysaccharide suitable for application in pharmaceutical technology. In the recent years, chitosan gel beads have been investigated as drug delivery system [1]. Many approaches have been developed to prepare the chitosan microparticles, such as by spray drying process [2], and coacervation/precipitation [3]. Protonation of the amino group allows the polymer to be solubilized in aqueous acids and to interact with negatively charged materials [4]. It is this functional group that enables the formation of chitosan micro/nanoparticles by crosslinking with tripolyphosphate [5].

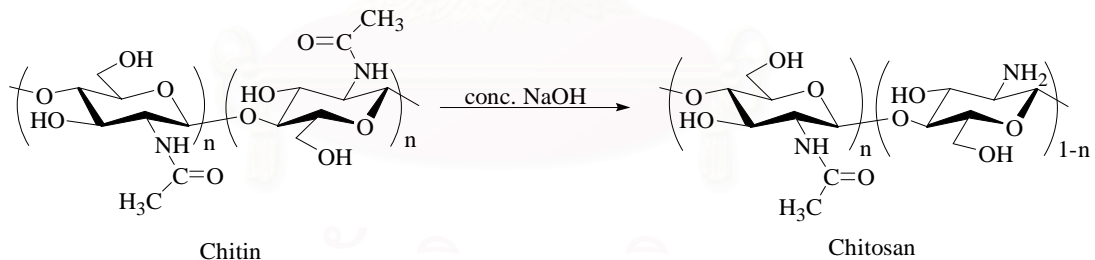


Figure 1.1 Chemical structure of chitin and chitosan

Ultrasonic atomization is a novel technique that can be utilized for the production of powders, granules or agglomerates from liquid suspensions. The principle of the nanoparticle generator used in this work is based on drying of atomized droplets through hot air. The ultrasonic atomizer is building the pressure waves in polymer solution. This pressure waves cause a lot of air bubbles and burst severely into fine cavitation. The polymer solution is therefore expanded into fine aerosol. When the aerosol comes into contact with hot air in a drying unit, the solvent evaporates; fine polymer particles are obtained (Figure 1.2).

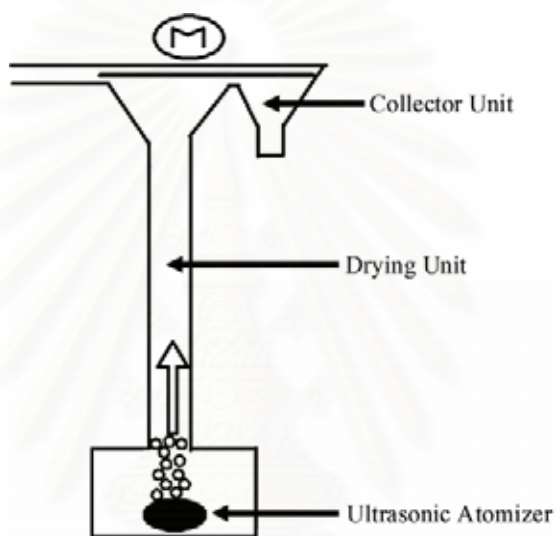


Figure 1.2 Schematic presentation of preparation of particles using ultrasonic atomization technique

So far, no information on chitosan particle formation by a generator equipped with an ultrasonic atomizer has been reported. Although a number of reports on nanoparticle formation for chitosan were presented, almost all of them were based on mixtures of chitosan and crosslinking chemicals. This work therefore focuses on preparing micro to nano sized particles of chitosan without any crosslinking chemicals. A particle generator equipped with an ultrasonic atomizer, a drying unit, and a charged-plate collector was designed under a cooperation with Ebase, a company based in Thailand. The preparation of chitosan particles loaded with lidocaine hydrochloride as a model drug was also investigated. Effect of specifications of chitosan such as molecular weight and degree of deacetylation on size of spheres and drug release were studied.

1.2 Objectives

The overall objective of this study is to explore the use of ultrasonic atomization to produce fine chitosan particle (micro to nanometers in size) as carriers for controlled release of lidocaine, a model drug compound. Effect of concentration and physicochemical properties such as degree of deacetylation and molecular weight of chitosan on the size and morphology of particles were studied. The lidocaine release from chitosan particles was evaluated by buffer incubation and simulated skin permeation study using shed snake skin and cellulose membrane.

1.3 Scope and work

1.3.1 Literature review of related works

1.3.2 Characterization of the chitosan samples such as molecular weight, degree of deacetylation and apparent viscosity

1.3.3 Preparation of chitosan and chitosan-lidocaine particles using ultrasonic atomization technique with parameters including degree of deacetylation, molecular weight of chitosan, and solution concentration

1.3.4 Particle characterization in terms of particle morphology, size, chemical analysis and powder x-ray diffraction

1.3.5 Evaluation of drug content and drug entrapment efficiency as a function of preparation parameters; molecular weight of chitosan and ratio of chitosan to lidocaine

1.3.6 *In vitro* lidocaine release study from chitosan particles at various weight ratios of chitosan to lidocaine in phosphate buffer

1.3.7 *In vitro* lidocaine release study under simulated skin permeation condition by using cellulose membrane and shed snake skin

1.3.8 Report preparation of the summarized results

CHAPTER II

THEORY AND LITERATURE REVIEW

2.1 Chitosan

Chitosan is the most abundant polysaccharide, in fact second only to cellulose. Chitosan is obtained by deacetylation of chitin. The main commercial sources of chitin are the shell wastes of shrimp, crab, lobster, krill, and squid. Chitosan [Poly- β -(1 \rightarrow 4)-2-amino-2-deoxy-D-glucose] is a hydrophilic cationic polymer prepared by deacetylation of chitin. Molecular structure of chitin and chitosan, similar to cellulose, are long linear chain molecules of (1-4) linked glycans as shown in Figure 2.1. Repeating unit in chitin is 2-acetamide-2-deoxy-D-glucose (*N*-acetylglucosamine), while for chitosan it is an mixture with the deacetylated form (glucosamine) [6]. Chitosan has degree of deacetylation between 70% and 90%. The molecular structure and properties of chitosan are affected by the degree of deacetylation.

Chitosan is reportedly hydrophilic, nontoxic, biocompatible, and biodegradable. Other properties include adsorption properties and anti-microbial properties. It is therefore considered to be suitable for application in pharmaceutical technology [7].

Chitosan is insoluble in water but soluble in diluted acidic solvents. Organic acids such as acetic, formic and lactic acids are used for dissolving chitosan. The most commonly used solvent is 1% acetic acid solution. Solubility of chitosan in inorganic acid solvent is quite limited. Chitosan is soluble in 1% hydrochloric acid but insoluble in sulfuric and phosphoric acids. Chitosan solution's stability is poor above pH 7 due to precipitation or gelation that takes place in alkali pH range. Chitosan solution forms a poly-ion complex with anionic hydrocolloid and provides gel. Its solubility depends on the presence of the free amine groups capable of being protonated by the acid medium. Certainly there would appear to be no need for the high level of deacetylation in order to induce solubility in acid solution. For example, chitosan having degree of deacetylation about 64% can be completely soluble [8].

The apparent viscosity of chitosan solution is dependent on the molecular weight, the concentration, the added salt concentration, and the temperature. The viscosity increases with an increase in molecular weight and concentration of chitosan, while the viscosity decreases with an increase in temperature. The addition of salts reduces the repelling effect of each positively charged ammonium unit on neighboring glucosamine unit. This effect results in a more random coil like conformation of the molecule and a decrease of the viscosity of chitosan solution [9].

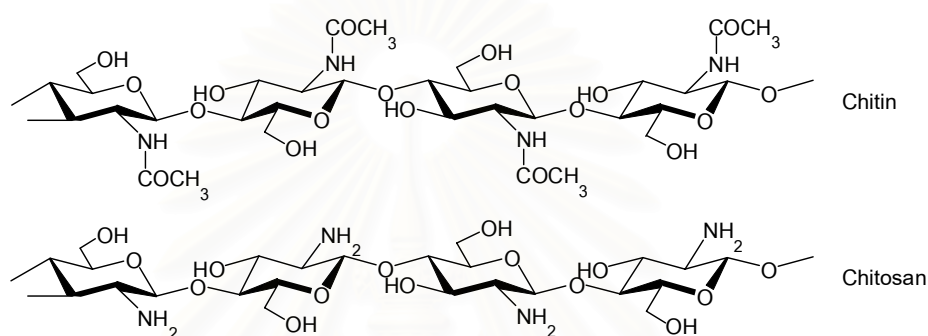


Figure 2.1 Structures of chitin and chitosan

2.2 Lidocaine hydrochloride

In this study, lidocaine hydrochloride was used as a model drug for drug release study from chitosan nanoparticles. Lidocaine hydrochloride (Figure 2.2), introduced in 1948, is probably the most widely used local anesthetic today, with applications ranging from infiltration anesthesia to field blocks, epidural anesthesia, spinal anesthesia and intra venous regional anesthesia [10]. Lidocaine and almost all local anesthetic agents are practically soluble in water.

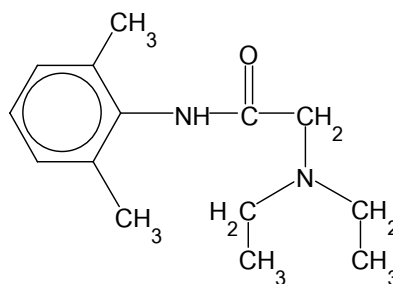


Figure 2.2 The structure of lidocaine hydrochloride [diethylamino-2,6-dimethyl-acetanilide hydrochloride]

Other properties of lidocaine hydrochloride are as follows:

Physical and Chemical Properties

- Physical state and appearance: Solid. (Powdered solid)
- Odor: Odorless
- Molecular Weight: 288.82 g/mole
- Color: White
- Melting Point: 77°C (170.6°F)

Stability and Reactivity Data

- Stability: The product is stable
- In compatibility with various substances: Reactive with oxidizing agents
- Corrosivity: Non-corrosive in presence of glass
- Polymerization: No

Toxicological Information

- Routes of Entry: Eye contact. Inhalation. Ingestion
- Toxicity to Animals: Acute oral toxicity (LD50): 220mg/kg
- Chronic Effects on Humans: The substance is toxic to the nervous system
- Other Toxic Effects on Humans:
 - Very hazardous in case of ingestion
 - Hazardous in case of skin contact (irritant), of inhalation
 - Slightly hazardous in case of skin contact (permeator)

2.3 Particle generator

2.3.1 Nano particle reactor

Nano particle reactor (Model NP-6010, EBASE Co., Ltd.) used in this study is equipped with an ultrasonic atomizer unit (Figure 2.3). The ultrasonic atomization is a novel technique to produce powders, granules or agglomerates from the suspensions. The principle of ultrasonic atomization is based on drying of atomized droplets through hot air. In this method, The ultrasonic atomizer unit represents a very specialized type of atomizing nozzle. Very fine droplets are generated without the use of high pressure or atomizing air. The droplets leave the nozzle with no feed velocity and their fall is affected only by gravity or, in this study, by charge-charge attraction in ambient conditions. Air assisted units are available which have no function in the atomization but solely in assisting with control of the polymer solution feed. The ultrasonic atomizer is building the pressure waves in the polymer solution. This pressure waves will cause a lot of air bubbles and burst severely into fine cavitation. The ultrasonic burst breaks up the polymer solution into fine aerosol. When the aerosol comes into contact with hot air in a drying unit, the solvent evaporates; fine polymer particles are obtained.

The following briefly describe the step of preparation of particle using the ultrasonic atomization technique. The first step is adding polymer solution into a solution reservoir. Then, the polymer solution is converted into droplets by the ultrasonic atomizer. After that the droplets enter a drying unit where solvent is evaporated. The drying unit consist of four computerized heaters placed one after the other. The dry particles was then flied up to a collector by electrostatic attracting force generated at a metal sheet. In case of chitosan, the collector unit is turned into negative charge so that the positively charged chitosan particles are attracted to the collector plate.

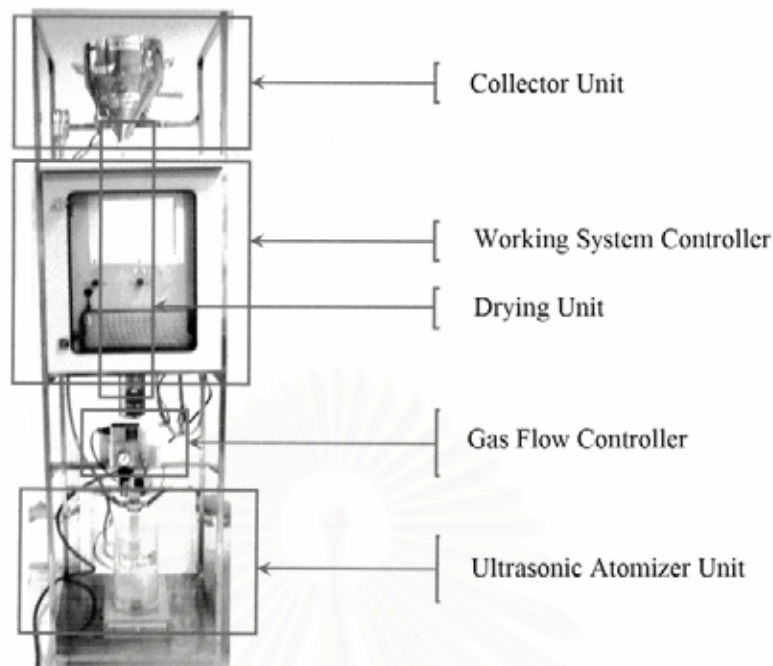


Figure 2.3 Presentation of Nano particle reactor equipped with an ultrasonic atomizer unit

2.3.2 Spray drying technique

Spray drying techniques (Figure 2.4) have been widely used in the pharmaceutical, chemical, and food industries. Its main use in the pharmaceutical industries includes drying of heat sensitive materials [11], improving the drug solubility [12, 13] or the flowability of particular excipients [14] and several other applications. Spray drying is a one step process to convert a liquid into a powder by spray drying a solution or a liquid dispersion through a nozzle in a drying chamber, where it comes in contact with hot air. The pharmaceutical industry utilized this technique to obtain powder, granules, agglomerates, and other more recent applications like microencapsulation and microsphere preparation [15].

The spray drying process encompasses the following four stages [16].

- a) Atomization of the feed into a spray
- b) Spray-air contact
- c) Drying of the spray
- d) Separation of the dried product from the drying gas

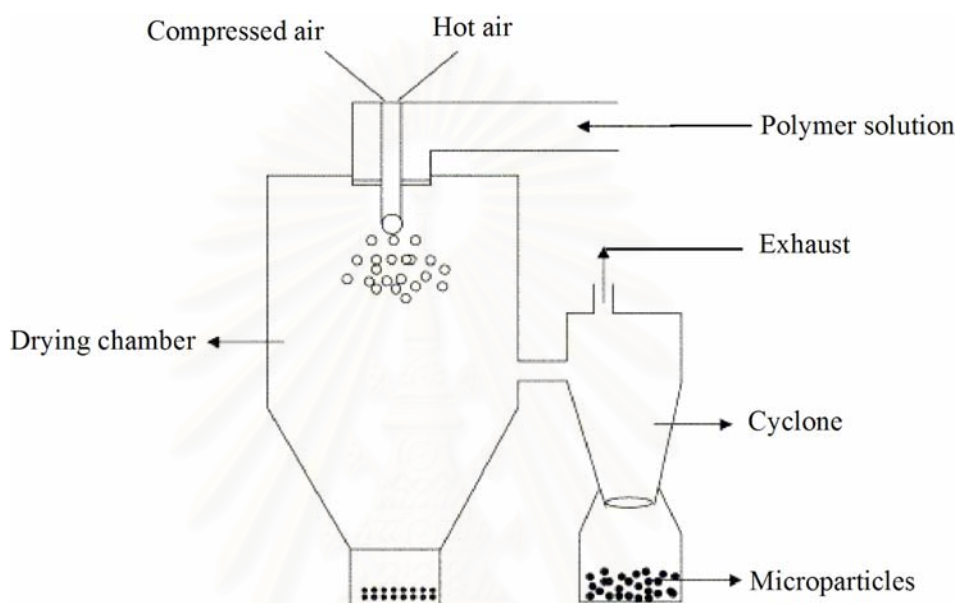


Figure 2.4 Schematic representation of spray drying technique [17]

2.4 Literature review on micro/nanoparticle preparation for controlled drug release

Lorenzo-Lamosa et al. [18] prepared the microencapsulated chitosan microspheres for colonic delivery of sodium diclofenac. Sodium diclofenac was entrapped into CS microcores by spray-drying and then, microencapsulated into Eudragit® L-100 and Eudragit® S-100 using an oil-in-oil solvent evaporation method. By spray-drying, CS microspheres of 1.8–2.9 μm sizes were prepared and efficiently microencapsulated into Eudragit® microspheres ranging in size between 152 and 223 μm to form the multireservoir system. Number of variables such as type and concentration of chitosan, the core/coat ratio and the type of enteric polymer have been investigated to optimize the microsphere properties.

M. Polakovic et al. [19] prepared lidocaine load poly(D,L-lactic acid) nanoparticles by emulsion-solvent evaporation method to investigate the releasing. The results indicated that lidocaine load poly(D,L-lactic acid) particles have sizes ranging from 250 to 820 nm. In addition, the rate of release correlated with the particle drug loading and was fastest at small particles with a low drug content. It was about four times slower at large particles with a high loading when the process of release took up to 100 h.

H.Q. Mao et al. [20] prepared chitosan–DNA nanoparticles using the complex coacervation technique. Important parameters such as concentrations of DNA, chitosan, sodium sulfate, temperature, pH of the buffer and molecular weights of chitosan and DNA have been investigated. At the amino to phosphate group ratio between 3 and 8 and chitosan concentration of 100 µg/mL, the particle size was optimized to 100–250 nm with a narrow distribution. Surface charge of these particles was slightly positive with a zeta potential of 112 to 118 mV at pH lower than 6.0, and became nearly neutral at pH 7.2. The chitosan–DNA nanoparticles could partially protect the encapsulated plasmid DNA from nuclease degradation.

S. Ramanathan et al. [1] prepared lidocaine load chitosan gel beads by dissolving the chitosan (molecular weight=2,000 kDa, degree of deacetylation=80) in 10% acetic acid. The results indicated that lidocaine was release continuously for 60 min.

S. Mitra et al. [21] have encapsulated doxorubicin–dextran conjugate in CS nanoparticles prepared by reverse micelle method. The surfactant sodium bis (ethylhexyl) sulfosuccinate (AOT), was dissolved in n-hexane. To 40 mL of AOT solution (0.03M), 100µL of 0.1% chitosan solution in acetic acid, 200 µL doxorubicin–dextran conjugate (6.6 mg/mL), 10 µL liquid ammonia and 10 µL of 0.01% glutaraldehyde solution were added with continuous stirring at room temperature. This procedure produced chitosan nanoparticles encapsulating doxorubicin–dextran conjugate solvent was removed by rotary evaporator and the dry mass was resuspended in 5 mL of pH 7.4 Tris–C buffer by sonication. To this, 1 mL of 30% CaCl solution was added dropwise to precipitate the surfactant as calcium salt of diethylhexyl sulfosuccinate. The precipitate was pelleted by centrifugation a 5,000 rpm for 30 min at 4°C. The pellet was discarded and the supernatant containing

nanoparticles was centrifuged at 60,000 rpm for 2 h to pellet the nanoparticles. The pellet was dispersed in 5 mL of pH 7.4 Tris–HCl buffer.

S.G. Kumbar et al. [22] have used the emulsion crosslinking method to prepare chitosan microspheres to encapsulate diclofenac sodium using three cross-linking agents viz, glutaraldehyde, sulfuric acid and heat treatment. Microspheres were spherical with smooth surfaces. The size of the microparticles ranged between 40 and 230 μm . Among the three cross-linking agents used, glutaraldehyde cross-linked microspheres showed the slowest release rates while a quick release of diclofenac sodium was observed by the heat cross-linked microspheres.

Y. Hua, et al. [23] prepared the silk peptide load chitosan-acrylic acid nanoparticles by polymerization method. Chitosan with molecular weight of 40, 80, 100, 200 and 300 kDa and degree of deacetylation of 90 was used in this study. The results indicated that the particles have sizes ranging from 50 to 400 nm. In addition, the silk peptide was release continuously for 10 days.

Y. Pan et al. [24] prepared the insulin-loaded chitosan nanoparticles by ionotropic gelation of chitosan with tripolyphosphate anions. Particle size distribution and zeta potential were determined by photon correlation spectroscopy. The ability of chitosan nanoparticles to enhance the intestinal absorption of insulin and the relative pharmacological bioavailability of insulin was investigated by monitoring the plasma glucose level of alloxan-induced diabetic rats after the oral administration of various doses of insulin-loaded chitosan nanoparticles. The positively charged, stable chitosan nanoparticles showed particle size in the range of 250–400 nm. Insulin association was up to 80%. The *in vitro* release experiments indicated initial burst effect, which is pH-sensitive. The chitosan nanoparticles enhanced the intestinal absorption of insulin to a greater extent than the aqueous solution of CS *in vivo*. After administration of 21 I. U./kg insulin in the chitosan nanoparticles, hypoglycemia was prolonged over 15h. The average pharmacological bioavailability relative to s.c. injection of insulin solution was up to 14.9%.

E.S.K. Tang et al. [4] prepared chitosan nanoparticles that used tripolyphosphate is cross-link agent using ultrasonication method. Chitosan with molecular weight of 146 kDa and degree of deacetylation of 96 was used in this study. The result indicated that

the size of particle have mean diameter of 382 nm which amplitude of ultrasonication depended on the diameter of chitosan particle.

M. Asada et al. [2] prepared chitosan-theophylline microparticles using spray drying technique, with the purpose to sustained release the drug. The physicochemical properties of the solid dispersions obtained were investigated by powder X-ray diffraction, differential scanning calorimetry, and dissolution rate analyses, with a view to clarify the effect of crystallinity on the dissolution rate. In addition, the interaction between the drug and the carrier was investigated by FT-IR analysis. The results indicated that the particles have sizes ranging from 4.6 to 5.6 μm . The powder X-ray diffraction intensity of the drug in the spray dried samples decreased with an increase in chitosan contents, which also caused changes from crystalline to amorphous forms. These results indicated that the system formed a solid dispersion. At pH 6.8, the release from the solid dispersion was sustained more than that from the physical mixtures.

A. Grenha et al. [25] prepared insulin loaded chitosan nanoparticles by ionotropic gelation method using tripolyphosphate is cross-link agent. Chitosan with degree of deacetylation of 86 was used in this study. The results indicated that particles have sizes ranging from 300 to 390 nm and lidocaine was released mostly at 75-80% within 15 min.

T. Schmitz et al. [26] have developed chitosan thiobutylamidine and evaluated as a novel tool for gene delivery. The conjugate, displaying 299.1 ± 11.5 mmol free thiol groups per gram polymer, formed coacervates with pDNA at a mean size of 125 nm and a zeta potential of +9 mV. Thiol groups, being susceptible for oxidation, were immobilized on the polymeric backbone of chitosan in order to introduce the property of extracellular stability and intracellular pDNA release by forming reversible disulfide bonds. The integrity of the new particles was compared to un modified chitosan under simulated physiological conditions. Within 10h, pDNA was completely released from chitosan DNA particles while only 12% were released from the thiomers-based particles. At pH7, the amount of thiol groups significantly ($p < 0.05$) decreased by more than 25% within 6 h. In contrast, in a reducing environment as found intracellularly, chitosan-thiobutyl amidine DNA nanoparticles dissociated continuously, liberating approximately 50% of pDNA within 3 h. Transfection studies performed in Caco2 cell culture evinced the highest efficiency for chitosan-thiobutyl

amidine DNA nanoparticles in combination with a glycerol stock solution. The combination of improved stability, enhanced pDNA release under reducing conditions, and higher transfection efficiency identifies chitosan-thiobutyl amidine as a promising new vector for gene delivery.

2.5 Controlled release system

The means by which a drug is introduced into the body is almost as important as the drug itself. Drug concentration at the site of action must be maintained at a level that provides maximum therapeutic benefit and minimum toxicity. The pharmaceutical developer must also consider how to transport the drug to the appropriate part of the body and, once there, make it available for use [27].

Controlled drug delivery occurs when a polymer is combined with the drug or other active agents in such a way that the active agent is released from the material in a predesigned manner.

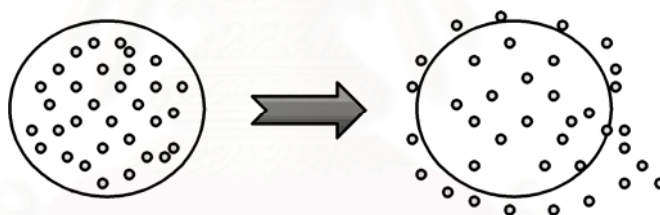


Figure 2.5 Presentation of controlled release system [28]

The drug can be released from the system by 3 mechanisms.

1) *Diffusion Controlled Release*

Diffusion occurs when drug molecules pass from the polymer matrix to the external environment. As the release continues, its rate normally decreases with this type of system, since drug has progressively longer distance to travel and therefore requires a longer diffusion time to release.

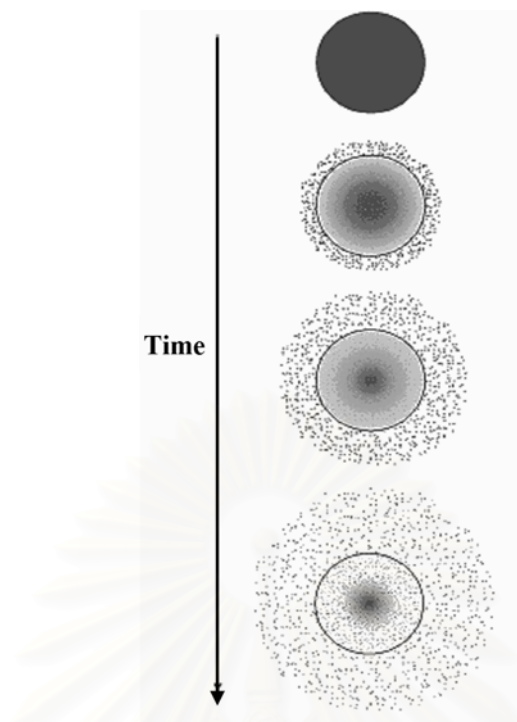


Figure 2.6 Presentation of diffusion controlled release [28]

2) *Swelling Controlled Release*

The swelling of the carrier increases the aqueous solvent content within the polymer matrix, enabling the drug to diffuse through the swollen network into the external environment. Most of materials used are based on hydrogel. The swelling can be triggered by a change in the environment surrounding such as pH, temperature, ionic strength, etc.

สถาบันวิทยบริการ
จุฬาลงกรณ์มหาวิทยาลัย

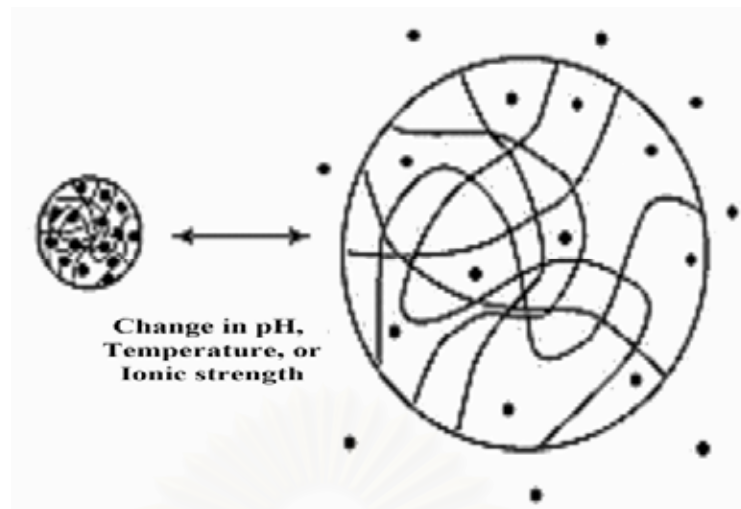


Figure 2.7 Presentation of swelling controlled release. [28]

3) *Erosion Controlled Release*

The drug can be released from the matrix due to erosion of polymers, which can be classified into 2 types.

Bulk erosion: The polymer degrades in a fairly uniform manner throughout the polymer matrix.

Surface erosion: The degradation occurs only at the surface of the polymer device.



Figure 2.8 Presentation of erosion controlled release-(a) bulk erosion and (b) surface erosion. [28]

2.6 Transdermal delivery systems

The skin is an important barrier to controlled drug delivery. Approaches for delivering drugs throughout the skin as well as recent advances in iontophoresis, ultrasound, chemical enhancers, and chemical treatment of drugs for transdermal delivery are discussed [29].

Transdermal delivery system is the results of sophisticated procedures, where technology prevailed over a well-known pharmacological component, resulting in the development of the system in a short time. Such development progressed through three stages, or generations, aimed at improving delivery and absorption, reducing patch size and making it easier to use. Furthermore, the therapeutic benefits of transdermal drug delivery systems are an important issue in the development of any drug products.

The advantages transdermal drug delivery are:

- Adaptability to drugs with a short half-life.
- Avoidance of variation in gastrointestinal absorption.
- By pass of the hepatic first pass metabolism.
- Good patient compliance.
- Production of sustained and constant plasma concentrations of drugs
- Reduction in repeated dosing intervals.
- Reduction of potential adverse side effects.
- Removal of transdermal drug delivery systems provokes an immediate decrease of drug plasma levels.
- Substitute for oral or parenteral administration in certain clinical situation (pediatrics, geriatrics, nausea, etc.)
- Suitable for drugs which produce a therapeutic response at very low plasma concentrations.

2.7 Franz' s cell apparatus

Franz' s cell (Figure 2.9) are used for *in vitro* study to quantify the release rate of drugs from topical preparation. In these systems, skin membranes or synthetic membranes may be used as barriers to the flow of drug and vehicle to simulate the biological system. The typical of franz' s cell has two chambers, one on each side of the

test diffusion membrane. A temperature-controlled solution is placed in one chamber and a receptor solution in the others. Drug permeation may be determined by periodic sampling and assay of the drug content in the receptor solution. Franz's cell is the most widely used apparatus to determine the drug release profile from the topical drug products because of the reliability and reproducibility. The test sample is placed in the donor phase, which was separated from the receptor phase by a semipermeable membrane. The suitable receptor medium is suggested to increase the drug solubility for detection of drug release by the ultraviolet spectroscopy or high-pressure liquid chromatography (HPLC) [30].

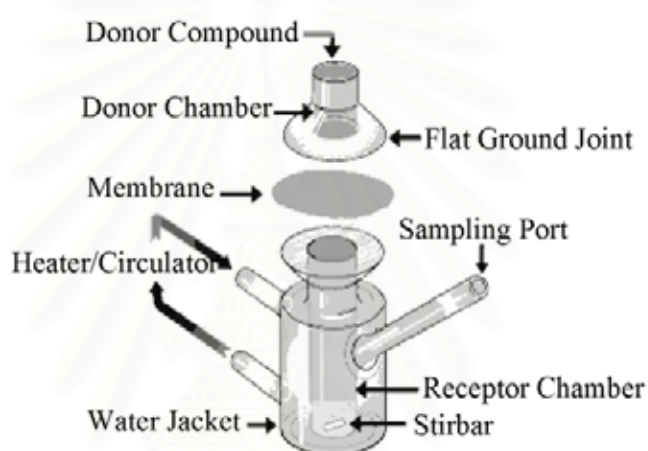


Figure 2.9 The components of Franz' s cell [31]

2.8 Skin sources

The difference of skin sources give the different results in percutaneous absorption, these differences are due to the physiology of the skin. The types of skin sources in percutaneous absorption studies were human skin, animal skin and artificial skin and skin cultures.

Human skin

The human skin is the most appropriate choice to predict the percutaneous absorption. In the literatures, the various regions of human skin were used to studies in percutaneous absorption, such as the abdominal skin studies on propranolol [32], bisoprolol [33] and nitrovasodilator drugs [34], the breast skin studies on lorazepam,

clanzepam [35] and triclosan [36] and the forearm skin study on capsaicin [37]. The fresh human skin can be obtained from surgery but the availability is limited. Fresh skin can be kept viable for some time allowing some metabolism of the test compound to take place. Since the stratum corneum consist of dead cells, human cadaver skin from autopsies can be used [38].

Animal skin

The animal skin cannot be directly corrected to human skin because animal skin differs from human skin in several ways. Most animals have furry skin and thickness of the stratum corneum is often thicker than in human skin. The choice of animal skin often depends upon ease of availability and the similar physiological to human skin. The percutaneous absorption has been determined in many animal species, including rats, mice, rabbits, guinea pigs, pigs and snakes. The animal skins that have been used in permeation studies showed in Table 2.1.

Table 2.1 The animal skins that have been used in permeation studies

Species	Permeant	References
Mice	Ketotifen fumarate	Kimura C. et al. 2007 [39]
	Bovine serum albumin	Xie Y. et al. 2005 [40]
	4-nerolidyl-cathecol	Cristina et al. 2002 [41]
Pig	Ketoprofen and propylene glycol	Bowen, Jenna L et al. 2006 [42]
	Moxifloxacin	Kerec M. et al. 2005 [43]
Snake	Ethyl nicotinate	Ngawhirunpat T. et al. 2004 [44]
	lidocaine	Kang L. et al. 2000 [45]

Shed Snake skin

Typically, shed snake skin penetration studies provide conservative estimation for human skin penetration since it is less permeable than human skin for most compounds [45]. Recently, the use of shed snake skin as membrane model for *in vitro* diffusion studies becomes attractive. It is important to have alternate biological or

synthetic membranes that mimic human thus, a single snake skin could provide multiple samples. Since snake skin lacks of hair follicles, the problems associated with the transfollicular route of penetration, which might be significant in mammalian skins, is overlooked.

However shed snake skin consists of three distinctive layers, beta-keratin-rich outermost beta layer, alpha-keratin and lipid-rich innermost alpha layer. Furthermore, the mesos layer shows three to five layers of cornified cells surrounding by intercellular lipids. Therefore, the mesos layer is similar to human stratum corneum. This mesos layer is also a major depot of lipids. The mesos layer and alpha layer are considered to be the main barrier to water penetration through the skin. Furthermore, water permeabilities of shed snake skins from normal snakes and scaleless skin are determined and showed that the existence of scales might not affect significantly the permeability of compounds through shed snake skin.



CHAPTER III

METHODS AND MATERIALS

3.1 Materials

Chitosan with \overline{M}_w of 75 kDa and %deacetylation degree (DD) of 94% was purchased from A.N. LAB Co., Ltd. Chitosan with \overline{M}_w of 150 kDa and DD of 90%, 82% and 76%, and chitosan with \overline{M}_w of 238 kDa and DD of 95% were purchased from Seafresh Chitosan (Lab) Co., Ltd. Finally, chitosan with \overline{M}_w of 47kDa and DD of 94% was prepared in the laboratory by inducing chain degradation of the chitosan (75 kDa) using an ultrasonic probe.

Lidocaine hydrochloride (LC-HCl) was purchased from S.M. Chemical Supplies Co., Ltd. Cellulose dialysis membrane with \overline{M}_w cut off at 3,500 Da was acquired from Spectrum Laboratories Inc. Shed snake skin of *Naja kaouthia* was donated by Queen Saovabha Memorial Institute.

The other reagents from Carlo Erba Reactifs SA are analytical grade such as acetic acid glacial, acetone, chloroform, citric acid, methanol, n-hexane, sodium hydroxide. In addition, sodium phosphate dibasic was manufactured by Sigma-Aldrich Laborchemikalien GmbH.

3.2 Characterization of chitosan samples

3.2.1 Molecular weight of chitosan

The molecular weight of chitosan was determined using GPC (Gel Permeation Chromatography, Water 600E). Columns used were Ultrahydrogel (molecular weight resolving range = 1,000-20,000,000 Da). Solvent is composed of 0.5 M acetic acid and 0.5 M sodium acetate in water (acetate buffer). This solvent was filtered through nylon 66 membrane with a pore size of 0.45 μm before use. Pullulans (molecular weight, 5,900-788,000 Da) were used as standards. The analyzed sample was prepared by dissolving 0.2% w/v of chitosan in the solvent and shaken at 100 rpm for

24 hour. It was then filtered with a 0.45 μm nylon 66 membrane. The injection volume was 20 μL . The column was set at 30°C and flow rate was 0.6 mL per min.

3.2.2 Solubility of chitosan

Determination of chitosan solubility consisted of the following five stages.

1. Preparation of chitosan solution (1% w/v) by dissolving in acetic acid (1% v/v) at room temperature with shaking for 24 h.
2. Dried the filter paper at 105°C for 2 h and weight the filter paper after place in desiccator for 30 min.
3. Chitosan solution was filter using the suction.
4. Lead the filter paper that has chitosan gel was dried at 105°C for 24 h and place in the desiccator for 30-60 min before weight.
5. The solubility of chitosan was determined using the following formula:

$$\text{Solubility (\%)} = 1 - \frac{(B - A)}{C} \times 100$$

where A is the weight of filter paper (g), B is the weight of filter part and filter paper after dried at 105°C for 24 h (g) and C is the initial weight of chitosan (g).

3.2.3 Degree of deacetylation

Degree of deacetylation (DD) is defined as the percentage of glucosamine residues in the chitosan chain. The DD was calculated based on UV absorption data obtained from UV-spectrophotometer SPECORD S100. First derivative UV-spectrophotometric method reported by Muzzarelli et al. in 1985 [46] was used after slight modification for determination of the DD of chitosan. This method permits a simple and time saving assay of *N*-acetylglucosamine residues in chitosan leading to increase precision and accuracy. The DD was determined using the following formula:

$$DD = \left[1 - \frac{\frac{A}{10W - 204A} + 161A}{161} \right] \times 100$$

where A is the concentration of *N*-acetyl-D-glucosamine (g/L); calculated from relation equation of a predetermined calibration curve, 204 is the molecular weight of *N*-acetyl-D-glucosamine unit, 161 is the molecular weight of D-glucosamine, and W is the sample weight (g) in 100 mL of 0.01 M of acetic acid.

3.2.4 Apparent viscosity

Viscosity, one of the important factors, which determines the quality and molecular weight of chitosan, was measured by using Brookfield viscometer DVII⁺. To determine the viscosity, chitosan solution was prepared by dissolving chitosan (1%w/v) in acetic acid (1%v/v). Undissolved residuals were removed by filtration with nylon cloth. The chitosan solution was kept in water bath at $25\pm 1^\circ\text{C}$ for 2 h before measuring the viscosity.

3.3 Preparation of low molecular weight chitosan by ultrasonication

Chitosan was degraded by high intensity ultrasonic processor (500 watt). to produce low molecular mass chitosan. First, 1.25 g chitosan (75 kDa) was dissolved in 500 ml of acetic acid (1% v/v). The mixture was shaken for 12 h. The chitosan solution was then filtered through nylon cloth to dispose of undissolved impurities. An ultrasonic processor with a 2.5 cm stainless steel probe (Figure 3.1) was used to sonicate the chitosan solution. The ultrasonic probe was set to apply pulsed ultrasound with 5 s 'on' and 2 s 'off' period for 2 h. The probe was immersed 6 cm into the sample during ultrasonication, which was carried out at specified amplitudes of 80. Final molecular weight of degraded chitosan was analyzed using GPC (Gel Permeation Chromatography, Water 600E). This chitosan solution was used for the preparation of chitosan particles.

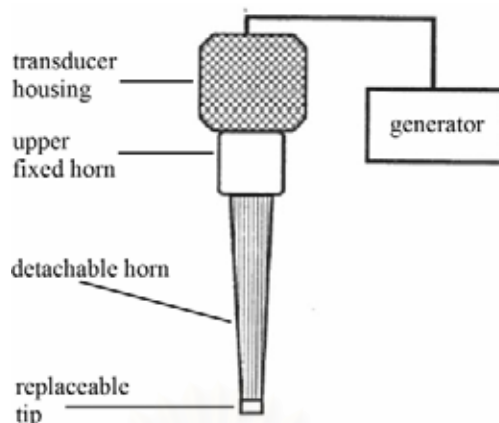


Figure 3.1 Schematic representation of ultrasonic probe

3.4 Particle preparation

The chitosan particles were prepared by using a nanoparticle reactor (NP-6010, EBASE Co., Ltd.) which was developed from the principle of ultrasonic atomization technique (Figure 1.2, in Chapter I). The chitosan solution (1% w/v) was prepared by dissolving in dilute acetic acid (1% v/v) at room temperature with shaking for 12 h. The solution was then filtered through nylon cloth to dispose of impurities. The filtrate was added into a solution reservoir at the base of the nanoparticle reactor. The reactor switch was then turned on. During the process, ultrasonic wave transformed the solution into aerosol. After that an aerosol came to drying unit. The fine particles were collected at an electronegative plate collector at the top of the reactor.

The preparation of lidocaine-loaded particles follows the method mentioned above, but with some modifications as follows. Chitosan-lidocaine solutions were prepared by adding a specified amount of lidocaine hydrochloride into the chitosan solutions under magnetic stirring at 100 rpm for 1 hour. This mixed solution was then used for particle preparation. The parameters studied for the particle preparation by using an ultrasonic atomization technique are shown in Table 3.1.

Table 3.1 The parameters studied for the particle preparation by using an ultrasonic atomization technique

Molecular weight (kDa)	47, 75, 150, 238
Degree of deacetylation (%DD)	90, 82, 76
Concentration (%w/v)	0.25, 0.5, 0.75, 1.5
Ratio of lidocaine:chitosan (w/w)	0.33:1, 0.5:1, 1:1

3.5 Characterization of particles

3.5.1 Microscopic analysis

The morphology and surface appearance of particles (before and after the drug loading) were examined by a scanning electron microscope or SEM (Model JSM-6301F LV JEOL, Japan). The sample was mounted onto an aluminum stub using double-sided carbon adhesive tape and coated with gold-palladium. Coating was achieved at 18 mA for at least 4 min. Scanning was performed under high vacuum and ambient temperature with beam voltage between 10-20 kV.

3.5.2 Particle size measurement

The size measurement of chitosan particles and chitosan-lidocaine particles were performed on a particle sizer (Zetasizer Nano ZS, Malvern Instruments), using He-Ne laser with 4.0 mW power at a 532 nm wavelength. Size calculation was based on DLS method as a software protocol. The scattering light was collected at an angle of 90° through fiber optics and converted to an electrical signal by an avalanche photodiode array (APDs). A known weight (10 mg) of samples were sonicated and run in triplicate with the number of runs set to 5 and run duration set to 10 seconds.

In addition, the mean particle size of chitosan particles was also determined from the scanning electron micrographs, in which the diameters of 100 randomly selected particles were measured by a digital software. The averaged particle size determined by SEM (Model JSM-6480 LV JEOL, Japan) was reported as the size of 'dry' particles.

3.5.3 Functional group analysis

The IR spectra of lidocaine hydrochloride, chitosan and lidocaine hydrochloride loaded chitosan matrices were examined using the potassium bromide disk (KBr) method with an infrared spectroscopy in the range of 4000-400 cm^{-1} (Infrared spectrometer Model FT-IR 1760X, Perkin Elmer, Germany).

3.5.4 Powder x-ray diffraction study

Lidocaine hydrochloride distribution within the particles was investigated by X-ray diffractometry (X-ray diffractometer Model JDX-8030, JEOL, Japan). The samples for X-ray diffraction studies were firmly packed into a cavity of a thin rectangular metal plate using two glass slides attached to the metal plate with adhesive tape. The first glass slide was then removed, and the prepared sample was taken to expose to the X-ray diffraction chamber. The X-ray diffraction patterns were recorded from 5° to 65° in terms of 2θ angle.

3.6 Evaluation of drug content and drug entrapment efficiency

3.6.1 Calibration curve of lidocaine for UV spectroscopy

Lidocaine hydrochloride 10 mg was accurately weighed and transferred into a 100 mL volumetric flask. The lidocaine was dissolved in distilled water; the solution was adjusted to volume, and used as stock solution. The stock solution was individually pipetted (4, 4.5, 5, 10, 15 and 20 mL) into a 50 mL volumetric flask by Transferpette® S (Einkanal-Pipette Single-channel pipette) and diluted to volume with distilled water. The final concentration of each solution was 80, 90, 100, 200, 300 and 400 $\mu\text{g/mL}$ accordingly.

The absorbance of known lidocaine concentration was determined by UV/visible spectrophotometer (Model S100) in a 1 cm cell at a wavelength of 262 nm [42]. The distilled water was used as blank medium. The absorbances and the calibration curves of lidocaine in distilled water are presented in Table 1B and Figure 1B, respectively, in Appendix B.

3.6.2 Determination of drug content

The lidocaine content in CS-LC-Ps were determined by distilled water extraction. A known weight (25 mg) of sample was pulverized and incubated in 100 mL of distilled water with magnetic stirring for 24 h. The suspensions were then centrifuged at 3000 rpm for 30 min. by IEC Centrifuge (Model MP4R). The supernatant solution was assayed for lidocaine contents by UV/visible spectrophotometer (Model S100) in a 1 cm cell at a wavelength of 262 nm and calculated from a calibration curve. The distilled water was used as blank medium. All samples were analyzed in triplicate. The lidocaine content was calculated from the following equations:

$$\begin{aligned} \text{Amount of lidocaine (g/g of CS - LC - Ps)} \\ = \frac{\text{Concentration of lidocaine (g/mL)}}{0.025 \text{ g of CS - LC - Ps}} \times 100 \text{ mL} \end{aligned}$$

3.6.3 Determination of drug entrapment efficiency (EE)

A known weight of CS-LC-Ps were suspended in distilled water. The suspension was centrifuged at 3000 rpm for 30 min at 25°C to separate the free drug in the supernatant from the drug incorporated in the particles. Concentrations of drug in the supernatant were determined by UV/visible spectrophotometer (Model S100). The amount of the drug incorporated in the particles was calculated by using the same equation used for determining the drug content. Then, the drug entrapment efficiency was calculated according to the following equation:

$$\%EE = \frac{\text{Lidocaine content in CS - LC - Ps from experiment}}{\text{Lidocaine content in CS - LC - Ps from theory}} \times 100$$

The drug entrapment efficiency was studied as a function of chitosan molecular weights (47, 75 and 150 kDa) and chitosan to drug weight ratios (CS:LC =1:0.33, 1:0.5, 1:1).

3.7 *In vitro* lidocaine release from chitosan nanoparticles

3.7.1 Preparation of buffer medium for drug release study

The phosphate buffer with pH of 7.4 was used as medium for drug release study. The buffer was composed of 0.2 M sodium phosphate dibasic (454.25 mL) and 0.1 M citric acid (45.75 mL) [47].

3.7.2 Calibration curve of lidocaine in buffer solution

In order to make a standard curve, 10 mg of lidocaine was accurately weighed into a 100 mL volumetric flask. The phosphate buffer was added to dissolve the lidocaine. The solution was adjusted to volume, and used as stock solution. The stock solution was individually pipetted (5, 10, 15, 20, 25, 30 and 35 mL) into a 50 mL volumetric flask, and diluted to volume with phosphate buffer pH 7.4. The final concentration of each solution was 100, 200, 300, 400, 500, 600 and 700 $\mu\text{g/mL}$ accordingly.

The absorbance of known lidocaine concentration was determined by UV/visible spectrophotometer (Model S100) in a 1 cm cell at a wavelength of 262 nm. The phosphate buffer (pH 7.4) was used as blank medium. The absorbances and the calibration curves of lidocaine in the buffer (pH 7.4) are presented in Table 2B and Figure 2B, respectively, in Appendix B.

3.7.3 *In vitro* drug release

Lidocaine release from particles was studied by incubating 0.25 g of CS-LC NPs in 500 mL of phosphate buffer (pH 7.4) at $37\pm 1^\circ\text{C}$ under stirred condition at 100 rpm. Samples of 1 mL was withdrawn at the time intervals of 1, 2, 3, 4, 5 and 6 h. An equal volume of the fresh buffer was replaced immediately after each sampling in order to keep a constant volume of the buffer in the vessel throughout the experiment.

Each sampling solution was filtered through nylon filters (0.45 μm , Whatman, England) and assayed for the drug released by measuring the absorbance by UV/visible spectrophotometer (Model S100) in a 1 cm cell at a wavelength of 262 nm. The phosphate buffer pH 7.4 was used as blank medium. The amount of lidocaine at any time intervals were calculated from the calibration curve for each buffer

medium. Each of the releasing values reported was based on an average of three determinations of each formulation. The amount of cumulative lidocaine release are presented in Table 1C, 2C and 3C, respectively, in Appendix C. The percentage of cumulative lidocaine release are presented in Table 1D, 2D and 3D, respectively, in Appendix D.

The amount of lidocaine release and the percentage of cumulative lidocaine release were calculated from the following equations:

$$\begin{aligned} \text{Amount of lidocaine release (g/g of CS - LC - Ps)} \\ = \frac{\text{Concentration of lidocaine (g/mL)}}{0.25 \text{ g of CS - LC - Ps}} \times 500 \text{ mL} \end{aligned}$$

$$\% \text{ Cumulative release} = \frac{\text{Amount of lidocaine from releasing (g/g of CS - LC - Ps)}}{\text{Amount of lidocaine before releasing (g/g of CS - LC - Ps)}} \times 100$$

3.8 *In vitro* study of drug permeation through shed snake skin and cellulose membrane

3.8.1 Drug permeation studies

Franz's cell was employed for *in vitro* drug permeation study (Fig. 3.2a and 3.2b). The membrane being studied was placed between the donor and receptor chambers. The upper donor chamber was filled with chitosan-lidocaine particles suspended in phosphate buffer at pH 5.6 (50 mg of CS-LC-Ps / 2 mL of phosphate buffer). The diameter of the Franz cell was 1.5 cm corresponding to an effectively permeable area of 1.77 cm². The receptor chambers contained 12 mL of phosphate buffer (pH 7.4) as the receptor fluid. The receptor compartment was equipped with a magnetic stirring bar and the temperature was kept at 37±1°C by circulating water through a jacket surrounding the cell body throughout the experiment. One milliliter of receptor fluid was withdrawn at 1, 2, 3, 4, 5 and 6 h. Fresh buffer was replaced after each collection. The absorbance of withdrawn sample was determined by UV/visible spectrophotometer (Model S100) in a 1 cm cell at a wavelength of 262 nm. The phosphate buffer pH 7.4 was used as blank medium.

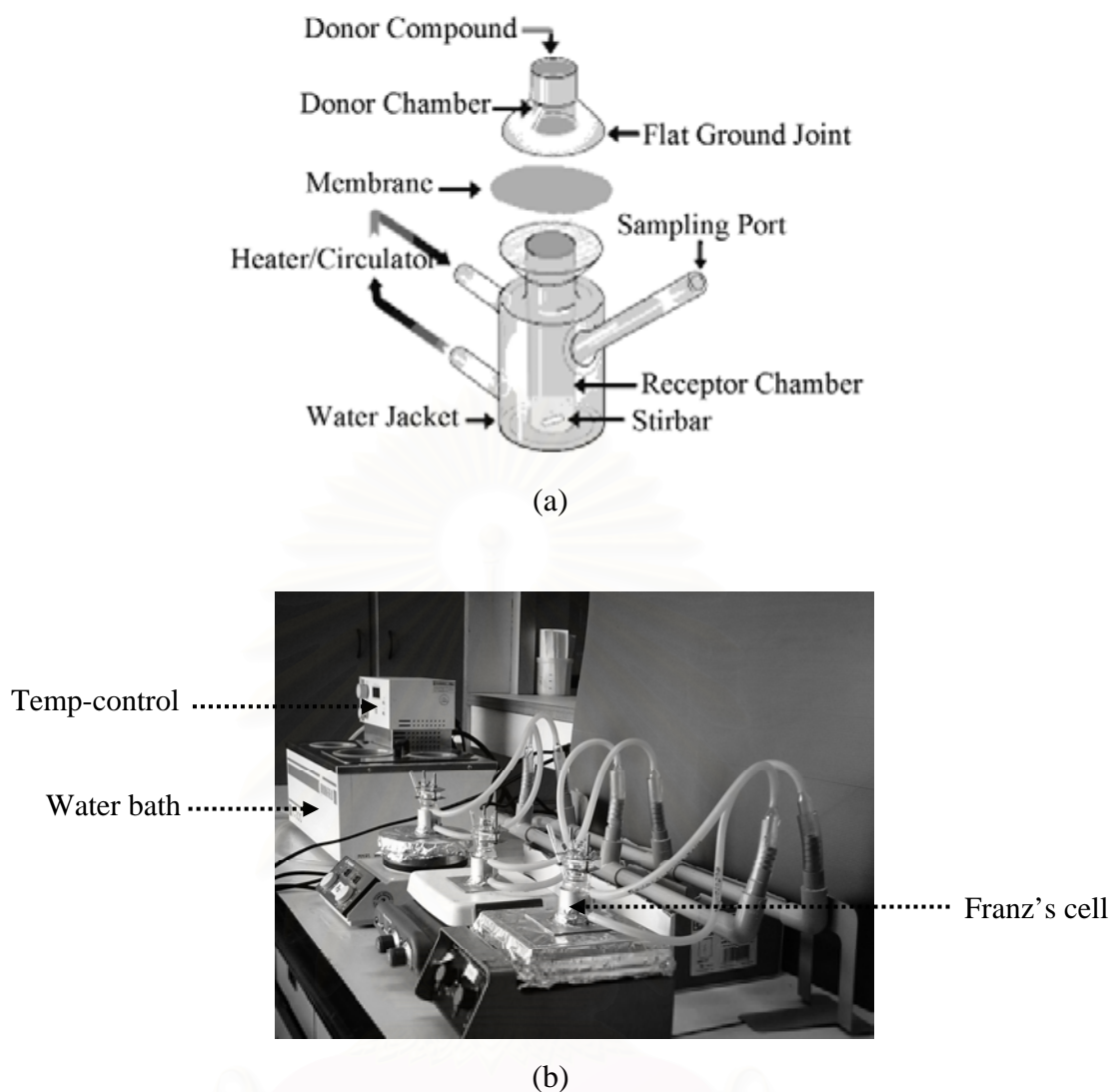


Figure 3.2 The components of Franz's cell [31] (a) and instrument set-up for permeation study (b)

The cumulative amount of drug permeated through a unit area of the membrane were calculated from the following equations:

$$Q_p = \frac{C_{LC} \times V_B}{A_M}$$

where Q_p is the cumulative amount of drug permeated through a unit area of shed snake skin or cellulose membrane ($\mu\text{g}/\text{cm}^2$), C_{LC} is the concentration of lidocaine permeated in receptor (g/mL), V_B is the volume of buffer pH 7.4 (12 mL for this experiment) in the receptor, A_M is the area of shed snake skin or cellulose membrane (1.77 cm^2 for this experiment).

The cumulative amount of drug permeated through a unit area of shed snake skin or cellulose membrane are presented in Table 1E-4E, in Appendix E and Table 1F-4F, in Appendix F, respectively.

The flux of lidocaine from CS-LC-Ps in the receptor compartment obtained from the slope of the linear correlation between cumulative amount of drug (Q_p) and time are presented in Figure 1E-8E, in Appendix E.

3.8.2 Buffer medium preparation

Preparation of phosphate buffer pH 7.4 was the same as the method used in the *in vitro* release study. Phosphate buffer pH 5.6 composed of 0.2 M sodium phosphate dibasic (290 mL) and 0.1 M citric acid (210 mL) [47].

3.8.3 Characterization of shed snake skin

Pretreatment of shed snake skin

Shed snake skin specimens from *Naja kaouthia* were selected as the representative of the stratum corneum, the major barrier to percutaneous drug absorption. All specimens were kept in the freezer. Prior to the experiment, they were thawed at room temperature and the dorsal part of the specimens were cut into pieces (2x2 cm² each in size). The samples were then soaked in the buffer medium (pH 7.4) for 12 h before used.

Morphological characterization of shed snake skin

The morphology and surface appearance of shed snake skin were examined by digital camera and scanning electron microscope (Model JSM-6480 LV JEOL, Japan), SEM.

Determination of shed snake skin thickness

The thickness of shed snake skin was determined using an electronic digital micrometer. The thickness reported was an average of ten measurements.

Determination of lipid content of shed snake skin

The lipid content determination was performed in order to correlate the permeation results with that of human skin. The shed snake skin (2x2 cm² each in

size) was dried at 50°C until constant weight. The specimen was then soaked in 0.1 N sodium hydroxide solution, chloroform-methanol (2:1v/v), acetone, and hexane, sequentially for 24 h in order to extract the lipid from the shed snake skin. Then the specimens were dried at 50°C until constant weight. The lipid content was calculated from the following equations:

$$\text{Lipid content (g)} = W_1 - W_2$$

$$\% \text{Lipid} = \frac{\text{Lipid content (g)}}{W_1} \times 100$$

where W_1 and W_2 are the weights of shed snake skin before and after extraction (g), respectively.

3.8.4 Characterization of cellulose membrane

Pretreatment of cellulose membrane

Prior to the experiment, the cellulose membranes were cut into pieces of 2×2 cm² each in size. They were then soaked in buffer medium (pH 7.4) for 12 hours before used.

Determination of cellulose membrane thickness

The thickness of cellulose membrane was determined using the electronic digital micrometer. The thickness reported was an average of ten measurement.

3.9 Statistical analysis

All measurements were performed in triplicate in each experiment. Results are presented as means ± SD. Statistical analysis was performed by one-way ANOVA using Microsoft Excel (Microsoft Corporation) with $P < 0.05$ considered to indicate statistical significance.

CHAPTER IV

RESULTS AND DISCUSSION

4.1 Characterization of chitosan

Table 4.1 General characteristics of chitosan (CS) used for particle preparation

Entry	Molecular weight of CS (kDa)	Degree of deacetylation (%DD)	Solubility (% w/w)	Viscosity (cps)
1	75	94	99	8
2	150	90	98	9
3	150	82	96	95
4	150	76	92	106
5	238	95	98	21

Solubility, molecular weight, and degree of deacetylation of chitosan samples used in this study are summarized in Table 4.1. The characterization methods are presented in Chapter 3. None of the chitosan samples dissolved completely in 1% acetic acid (1 g of chitosan in 100 mL of acetic acid solution). Residues of about 1-8% (w/w) were found on the filter papers during the solubility test. The insoluble residues were possibly ultra-high molecular weight chitosan chains and impurities from manufacturers. The %DDs were determined by UV spectrophotometry method, and varied from 76 to 95%. It seems that the solubility also decreased from 98% (*Entry 2 and 3*) to 92% (*Entry 4*) when %DD decreased to 76%, due to the increased content of *N*-acetyl glucosamine units in the polymer chain. From the data obtained, it was found that the viscosity depends more significantly on the degree of deacetylation than the molecular weight and of chitosan. The viscosity was increased by a decrease in the %DD from 94 (*Entry 1*) to 76% (*Entry 4*). For the samples having similar %DDs of 94-

95% (*Entry 1 and 5*), their viscosity values were found to be 8 and 21 cps, depending on the molecular weight of 75 and 238 kDa, respectively.

The ultrasonication of CS with molecular weight of 75 kDa was carried out in order to produce a low molecular weight sample. Viscosity results of the degraded samples are shown in Table 4.2. The result demonstrated that, at a fixed sonicating time of 1 h, the viscosity of the sonicated chitosan decreased with increasing an amplitude of ultrasonic processor, as reported by Tang et al. [4]. The viscosity decreases due to partial degradation of CS by acetic acid solutions. In this work, this method was used to obtain CS having low molecular weight of 47 kDa as determined by GPC technique. This low molecular weight CS was used in the preparation of chitosan particles.

Table 4.2 Viscosity and molecular weight of chitosan upon changing the amplitude of ultrasonication at a fixed period of 1 h (chitosan concentration = 0.25%w/v, 75 kDa)

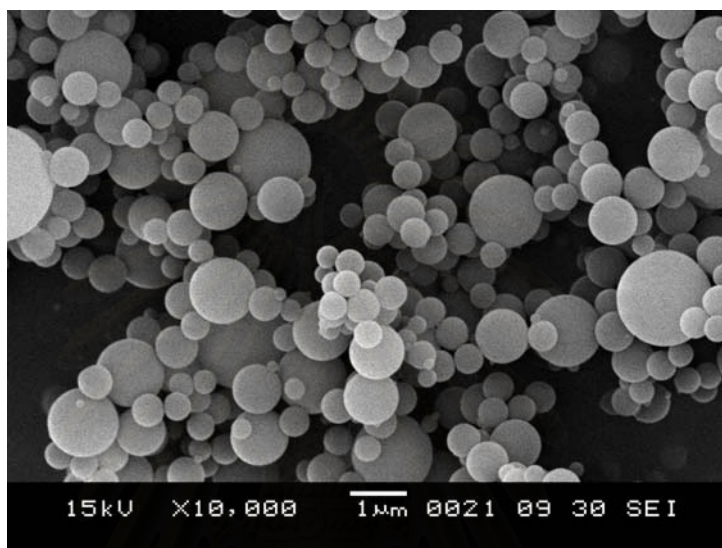
%Amplitude	Duration of ultrasonication (h)	Viscosity (cps)	\overline{M}_w (kDa)
0	1	5.91	75
20	1	5.82	-
40	1	5.70	-
60	1	5.52	-
80	1	5.40	47

4.2 Preparation of chitosan particles and lidocaine association

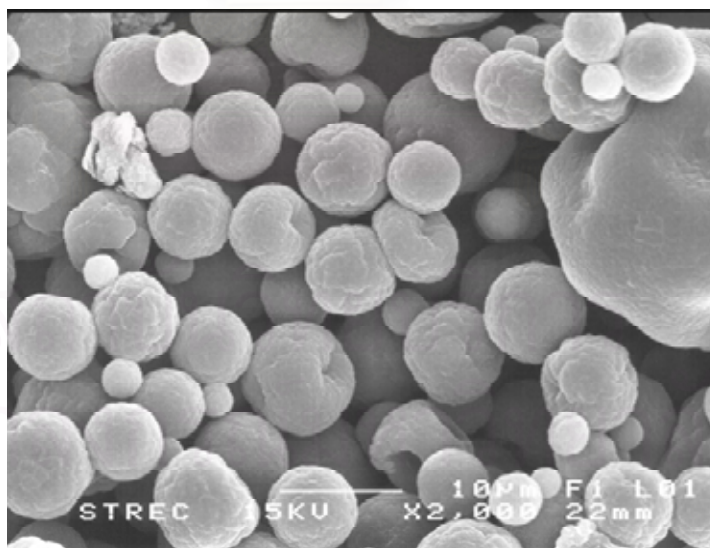
Chitosan particles were prepared by using the nanoparticle generator which was developed from the principle of ultrasonic atomization technique using chitosan solution in acetic acid. The particles appeared as white dust covering the collecting plate and side walls of the equipment. The collected yield of the particle was $57 \pm 6\%$ (averaged from three experiments) as compared to the amount of initial chitosan used. Only particles that stayed at the electrostatic plate and the main receiving channel were recovered.

4.2.1 Comparison of particles morphology as produced from ultrasonic atomization and spray dry technique

The chitosan particles prepared by ultrasonic atomization technique were spherical and had smooth surface. In case of chitosan particles prepared by spray dry, the particles had distinctly rough surface (Figure 4.1).



(a)



(b)

Figure 4.1 Scanning electron micrographs of chitosan particles prepared by ultrasonic atomization technique (a) and spray dry (b) produced from CS molecular weight of 75 kDa with 0.5% CS (w/v)

4.2.2 Physical characterization of particles

To monitor the shape and the surface structure of CS-Ps, the samples were analyzed by scanning electron microscopy (SEM). The surface morphological appearance of chitosan particles was compared with the CS-LC-Ps (Figure 4.2). Without lidocaine, the CS-Ps were spherical (Figs. 4.2a and 4.2b). Roughness on the surface could be clearly seen at high magnification (Figs. 4.2c-d, and 4.3a-c). In case of lidocaine containing particles, the surface of some CS-LC-Ps exhibited rough feature that was possibly related to the incorporated lidocaine on the particle surface. Upon detailed observation, it was found that not all CS-LC-Ps possessed this distinct roughness.

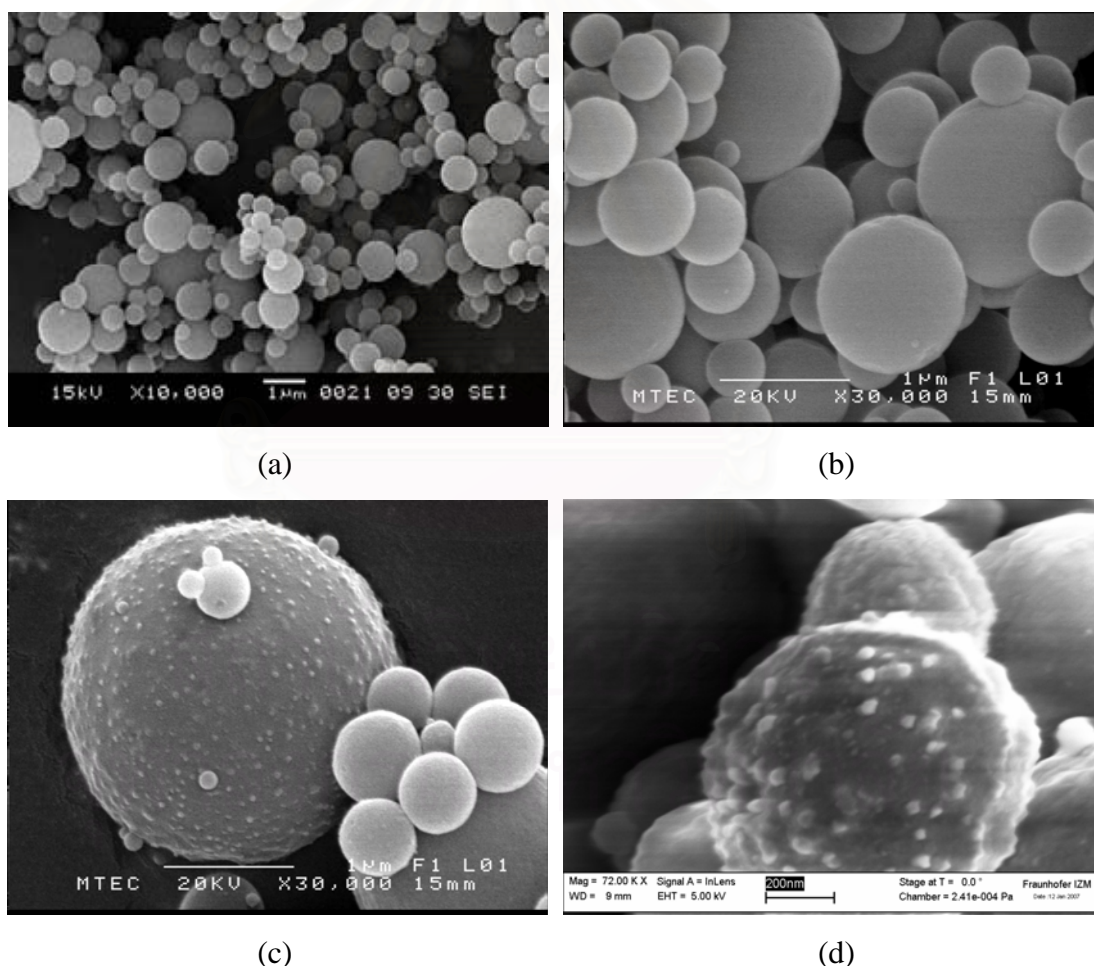


Figure 4.2 Scanning electron micrographs of blank CS-Ps (a and b), CS-LC-Ps (LC:CS = 0.5:1) (c), and CS-LC-Ps (LC:CS = 1:1) (d), produced from 0.5% CS solution (CS molecular weight = 75 kDa)

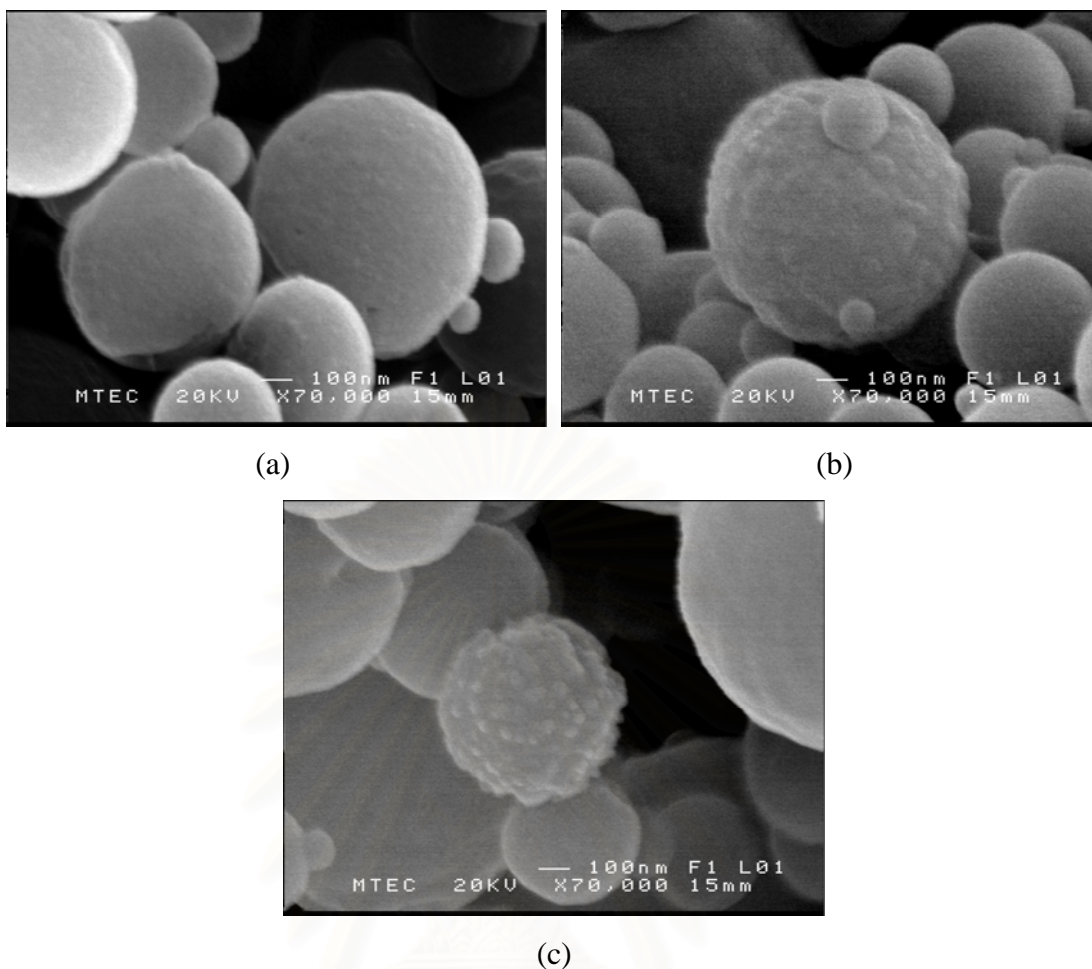


Figure 4.3 Scanning electron micrographs of CS-LC-Ps (LC:CS = 0.33:1) (a), CS-LC-Ps (LC:CS = 0.5:1) (b), and CS-LC-Ps (LC:CS = 1:1) (c), produced from 0.25% CS solution (CS molecular weight = 47 kDa)

Spherical particles were formed using an ultrasonic atomization technique. The particle size was determined by size measurement from scanning electron micrographs and by a particle sizer. The SEM technique was used to measure the size of dry particles, while the particle sizer was performed on hydrated samples. It is noteworthy that the particle sizes measured by the particle sizer are mostly higher than the size estimated from the SEM particularly because of the high swelling capacity of chitosan particles. Effect of concentration and physicochemical properties such as degree of deacetylation, molecular weight of chitosan and chitosan to drug mass ratio on the particle size were studied.

The sizes of CS-Ps obtained from SEM and the particle sizer upon varying the molecular weight of chitosan are presented in Table 4.3. SEM analysis revealed that, at

a fixed chitosan concentration, the averaged particle size tended to increase but not statistically significant ($p > 0.05$) when the molecular weights increased from 47 to 150 kDa (CS conc. = 0.25%) and from 75 to 238 kDa (CS conc. = 0.5%). It was, however, found that, the particle size obtained from the particle sizer significantly increased from 553 ± 96 to $1,041 \pm 156$ nm as the molecular weight increased from 75 to 238 kDa ($p < 0.05$). The observed change in particle size can be attributed to increased viscosity that was caused by the polymer with high molecular weight. As the viscosity increased the droplet size formed during atomization also increased, thus resulting in size increase.

Table 4.3 Effect of molecular weight on particle size of CS-Ps

MW (kDa)	DD (%)	CS conc. (%w/v)	Particle size ^a (nm) \pm SD	Particle size ^b (nm) \pm SD	PDI ^b
47	94	0.25	432 ± 176	250 ± 12	0.795
75	94	0.25	464 ± 199	417 ± 39	0.122
150	90	0.25	465 ± 259	530 ± 235	0.562
			$p = 0.4595593$	$p = 0.11661695$	
75	94	0.5	556 ± 252	553 ± 96	0.964
150	90	0.5	563 ± 222	877 ± 108	0.849
238	95	0.5	607 ± 171	$1,041 \pm 156$	0.241
			$p = 0.2024234$	$p = 0.00756634$	

^a Particle size as measured by SEM, ^b Particles size as measured by particle sizer

When changing %DD of the chitosan from 76 to 90% (at a fixed molecular weight of 150 kDa), not significant change of particle size was obtained from SEM analysis (Table 4.4). Analysis by the particle sizer, however, indicated that the %DD significantly affected the size of hydrated chitosan particles ($p < 0.05$). This can be explained by the fact that increasing %DD resulted in the decrease of solution viscosity, and therefore led to smaller particle size.

Table 4.4 Effect of %DD on particle size of CS-Ps

MW (kDa)	DD (%)	CS Conc.(%)	Particle size ^a (nm) ± SD	Particle size ^b (nm) ± SD	PDI ^b
150	76	0.5	619 ± 290	1,137 ± 122	0.125
150	82	0.5	578 ± 320	903 ± 85	0.184
150	90	0.5	563 ± 222	877 ± 108	0.849
			p = 0.344425	p = 0.04464962	

^a Particle size as measured by SEM, ^b Particles size as measured by particle sizer

The effect of chitosan concentration on particle size at a fixed chitosan molecular weight can be considered in Table 4.5. It can be clearly seen that the particle was significantly affected by the CS concentration from 0.25 to 1.5%w/v ($p < 0.05$). This can be simply explained by the fact that as the CS concentration increased the mass of CS in atomized droplets also increased. Moreover the CS concentration was the only factor that significantly affected the particle size in both dry and hydrated states.

Table 4.5 Effect of chitosan concentration on particle size of CS-Ps

MW (kDa)	DD (%)	CS Conc.(%)	Particle size ^a (nm) ± SD	Particle size ^b (nm) ± SD	PDI ^b
75	94	0.25	464 ± 199	417 ± 28	0.122
75	94	0.50	556 ± 252	553 ± 96	0.964
75	94	0.75	595 ± 239	999 ± 104	0.543
75	94	1.50	798 ± 416	1,520 ± 153	0.161
			p = 3.572 x 10 ⁻¹⁴	p = 5.004 x 10 ⁻⁷	

^a Particle size as measured by SEM, ^b Particles size as measured by particle sizer

The effect of chitosan to lidocaine mass ratio on particle size was studied as presented in Table 4.6. At a fixed molecular weight (MW) of CS and concentration, the size of CS-LC-Ps significant increased with the increasing drug content was obtained from SEM analysis ($p < 0.05$). Yet, in case of data obtained from the particle sizer, it

indicated that the drug content did not significantly affect the size of CS-LC-Ps ($p > 0.05$) when the drug content was between 0.33:1 to 1:1.

Table 4.6 Effect of lidocaine to chitosan mass ratio on the particle size of CS-LC-Ps

MW (kDa)	DD (%)	CS Conc. (%)	LC:CS (w/w)	Particle size ^a (nm) \pm SD	Particle size ^b (nm) \pm SD	PDI ^b
75	94	0.5	0.33:1	499 \pm 231	1025 \pm 188	0.292
75	94	0.5	0.5:1	663 \pm 381	1131 \pm 164	0.197
75	94	0.5	1:1	679 \pm 321	1301 \pm 283	0.204
				$p = 7.204 \times 10^{-5}$	$p = 0.35609822$	
47	94	0.25	0.33:1	442 \pm 156	706 \pm 78	0.052
47	94	0.25	0.5:1	486 \pm 277	708 \pm 185	0.096
47	94	0.25	1:1	669 \pm 495	883 \pm 117	0.121
				$p = 5.61 \times 10^{-6}$	$p = 0.15946032$	

^a Particle size as measured by SEM, ^b Particles size as measured by particle sizer

In addition, the effect of molecular weight on particle size was studied as presented in Table 4.7. at a fixed chitosan concentration and chitosan to drug ratio, the size of CS-LC-Ps as obtained by SEM significant increased with the increasing chitosan molecular weight ($p < 0.05$), but not the case for the hydrated particle size reported from particle sizer analysis in which the p value was higher than 0.05.

Table 4.7 Effect of chitosan molecular weight on the particle size of CS-LC-Ps

MW (kDa)	DD (%)	CS Conc. (%)	LC:CS (w/w)	Particle size ^a (nm) \pm SD	Particle size ^b (nm) \pm SD	PDI ^b
47	94	0.25	0.5:1	486 \pm 277	708 \pm 185	0.096
75	94	0.25	0.5:1	525 \pm 261	771 \pm 70	0.059
150	90	0.25	0.5:1	709 \pm 335	777 \pm 23	0.117
				$p = 1.392 \times 10^{-7}$	$p = 0.69425979$	

^a Particle size as measured by SEM, ^b Particles size as measured by particle sizer

4.2.3 Interaction between lidocaine and chitosan systems

The IR spectrum of the chitosan-lidocaine particles (CS-LC-Ps), lidocaine (LC) and chitosan particles (CS-Ps) were investigated by FTIR spectroscopy (Figure 4.4). Peak assignments are shown in Table 4.8. Interaction between lidocaine and chitosan was determined by comparing the IR transmission signals of pure components with the mixed system. All major peaks present in the pure component are found in the mixed system. In addition the O-H stretching band with a peak at $3,399\text{ cm}^{-1}$ obtained from CS-LC-Ps (Figure 4.4(a)) expanded to a lower wave number than that found in the pure component. This indicated additional hydrogen bonding between the incorporated LC and CS chain, which contained a high number of amino ($-\text{NH}_2$) and hydroxyl ($-\text{OH}$) groups.

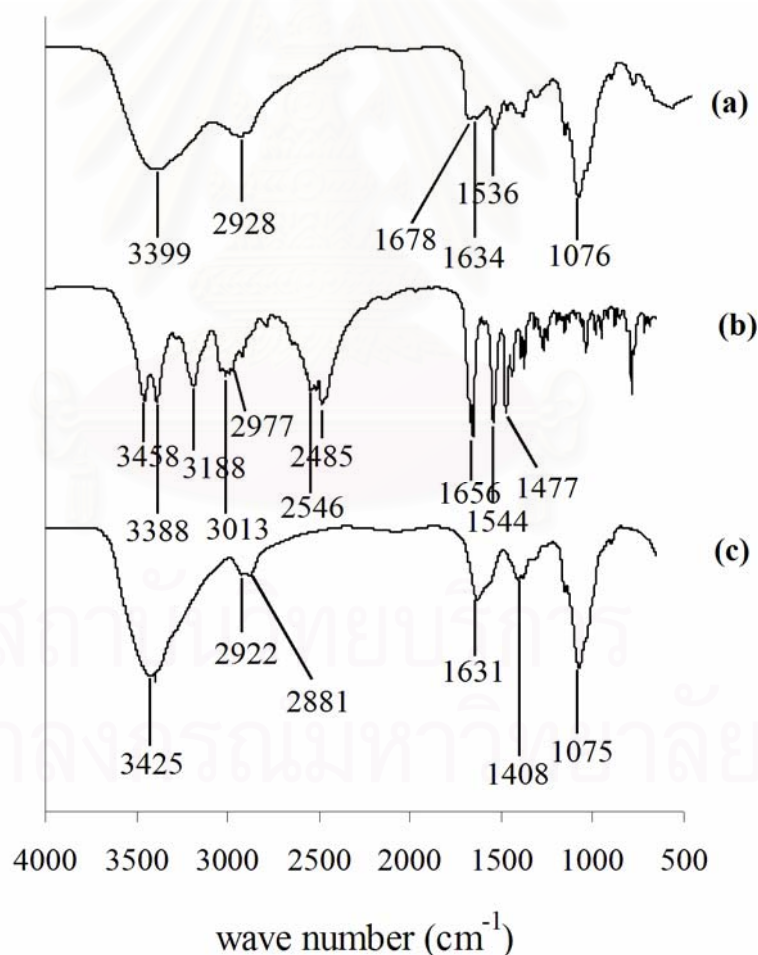


Figure 4.4 FT-IR spectra of CS-LC-Ps (LC:CS = 1:1) (a), lidocaine hydrochloride (b), and CS-Ps (c)

Table 4.8 Peak position and assignment of CS-LC-Ps (a), LC (b) and CS-Ps (c)

Sample	Peak position (cm ⁻¹)	Assignment
CS-LC-Ps (a)	1076	C-O stretching of ether
	1536	N-H bending of amide
	1634	C=O stretching of amide
	1678	C=O stretching of amide
	2928	C-H stretching of alkane
	3399	O-H stretching
LC (b)	1477	C=C stretching of aromatic
	1544	N-H bending of amide
	1656	C=O stretching of amide
	2485, 2546	N-H stretching of amine
	2977	C-H stretching of alkane
	3013	=C-H of aromatic
CS-Ps (c)	3188, 3388, 3458	O-H stretching
	1075	C-O stretching
	1408	C-H bending of aromatic
	1631	C=O stretching of amide
	2881, 2922	C-H stretching of alkane
	3425	O-H stretching

4.2.4 Degree of crystallinity of lidocaine in matrix particles

Figure 4.5 showed X-ray powder diffraction patterns of CS-LC-Ps, lidocaine hydrochloride and CS-Ps. As shown in Figure 4.5 (b) and (c), lidocaine has specific sharp peaks and chitosan has a broad peak, indicating the presence of crystalline and amorphous structures, respectively. When lidocaine was mixed into the chitosan

particles (Figure 4.5(a)), the sharp crystalline peaks disappeared. This could be explained that lidocaine dispersed among the chitosan chains and was not in the crystalline form.

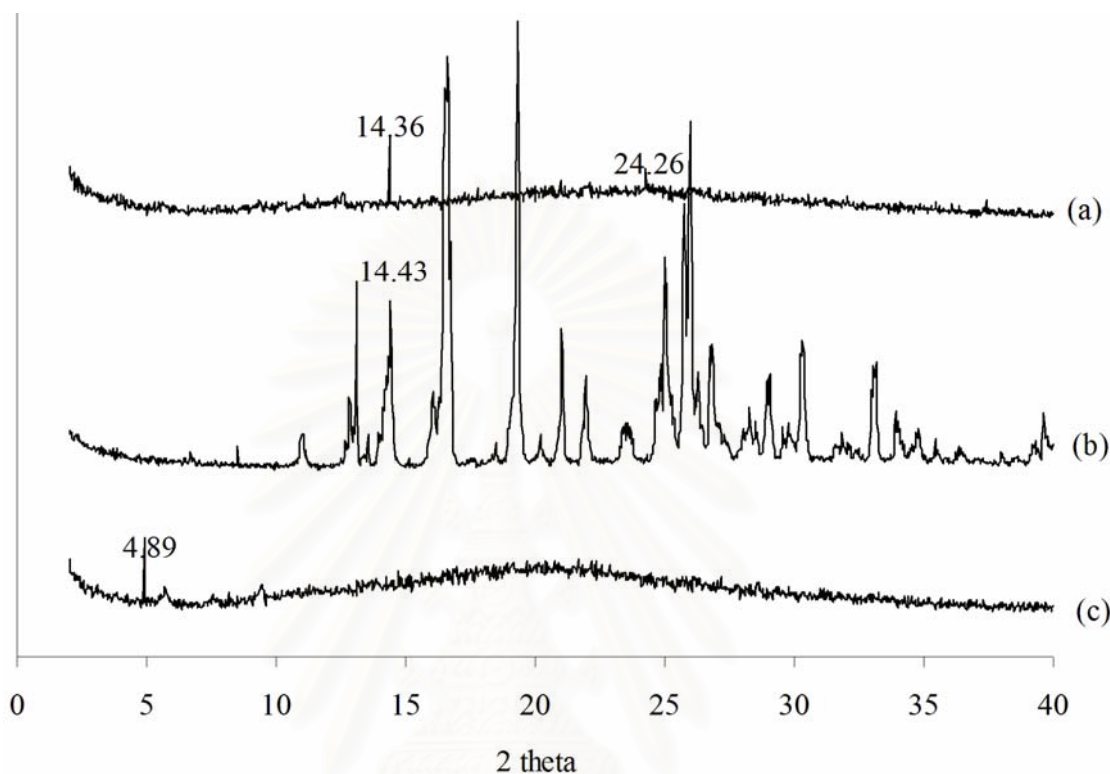


Figure 4.5 X-Ray diffractograms of CS-LC-Ps (LC:CS = 1:1) (a), lidocaine hydrochloride (b), and CS-Ps (c)

4.3 Evaluation of drug entrapment efficiency in chitosan particles

The content of drug within CS-LC-Ps was analyzed using UV/visible spectrophotometry. The lidocaine content was determined from the supernatant.

At a fixed chitosan molecular weight and chitosan concentration (Table 4.9), the lidocaine content within CS-LC-Ps was found to increase with the increasing of feed lidocaine amount from 0.25 to 0.50 g/g of CS-LC-Ps (Entry A-C and D-F). The contents of lidocaine in these particles were varied from 0.1901-0.3505 g and entrapment efficiencies (%EE) were between 70-91%. It seemed that as the feed LC content increased, %EE somewhat decreased. It was possible that the LC content of 0.50 g/g of CS-LC-Ps were approaching the saturated amount in the CS matrix.

Table 4.9 Lidocaine content and entrapment efficiency (%EE) at different lidocaine to chitosan mass ratios

Entry	Ratio of LC:CS (w/w)	Lidocaine content (g/g of CS-LC-Ps)		%EE
		Theoretical	Experimental	
A ^a	0.33:1	0.25	0.1901 ± 0.0024	76
B ^a	0.5:1	0.33	0.2578 ± 0.0118	78
C ^a	1:1	0.50	0.3477 ± 0.0166	70
D ^b	0.33:1	0.25	0.2255 ± 0.0008	90
E ^b	0.5:1	0.33	0.3012 ± 0.0085	91
F ^b	1:1	0.50	0.3505 ± 0.0006	70

^acondition: MW of CS = 75 kDa; CS conc. = 0.5%CS

^bcondition: MW of CS = 47 kDa; CS conc. = 0.25%CS

At a fixed chitosan concentration and chitosan to drug ratio (Table 4.10), the lidocaine content within CS-LC-Ps was found to decrease with the increasing of chitosan molecular weight. The entrapment efficiency also decreased from 91 to 48% when the molecular weight of CS increased. This can be understood by the fact that at high molecular weight chain entanglement and structural network are enhanced due to an increase of the inter-molecular hydrogen bonding of chitosan chains. This results in denser polymer networks in which lidocaine can hardly penetrate.

Table 4.10 Lidocaine content and entrapment efficiency (%EE) at different the chitosan molecular weights (CS conc. = 0.5%CS)

Entry	Mw of CS (kDa)	Ratio of LC:CS (w/w)	Lidocaine content (g/g of CS-LC-Ps)		%EE
			Theoretical	Experimental	
G	47	0.5:1	0.33	0.3012 ± 0.0085	91
H	75	0.5:1	0.33	0.1877 ± 0.0012	57
I	150	0.5:1	0.33	0.1577 ± 0.0088	48

4.4 Drug release study of chitosan particles in phosphate buffer medium

The content of lidocaine in CS-LC-Ps was analyzed using spectrophotometry method. The cumulative drug release from the CS particles having different drug contents were plotted as a function of time. The molecular weight of CS was fixed at 47 kDa and the concentration of CS solution was fixed at 0.25%w/v in all cases. Results indicated that the amounts of drug release was increased with increasing the drug to chitosan ratio (Figure 4.6 and Appendix B). The cumulative amounts of drug release from the CS-LC-Ps during the period of 6 h were 0.2156, 0.2808 and 0.3306 g/g of CS-LC-Ps for LC:CS mass ratio of 0.33:1, 0.5:1 and 1:1, respectively.

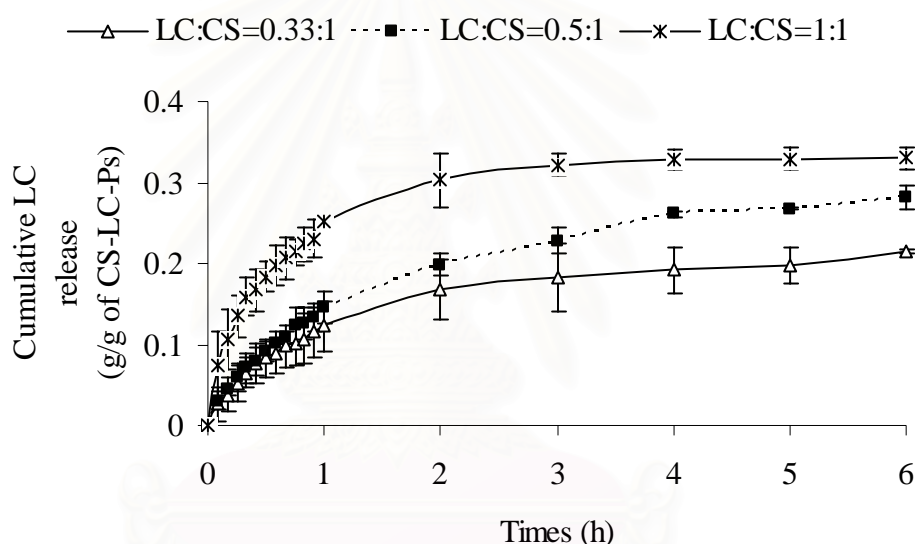


Figure 4.6 Comparison of cumulative LC release of CS-LC-Ps having different chitosan to drug ratios (CS: MW = 47 kDa, conc.= 0.25%). Error bars indicate the range of experimental reading obtained (sample number, $n = 3$).

The percentage of cumulative lidocaine release from CS-LC-Ps with the three chitosan to drug ratio were compared in Figure 4.7 (Appendix C). The present results demonstrate that the lidocaine release shows an increase of percentage of cumulative drug release with incubation time. The percentage of release from the CS-LC-Ps during the period of 6 h were 96, 93 and 94% for lidocaine to chitosan mass ratio of 0.33:1, 0.5:1 and 1:1, respectively. Moreover, up to 92% of lidocaine was continuously released from the prepared particles before reaching the plateau within the period of 3 h. The result from this study was somewhat different to the report of Maestrell, F. et al.

(2006) [48] for the preparation of hydroxypropylcyclodextrins-chitosan nanoparticles by ionic crosslinking of chitosan with sodium tripolyphosphate. They indicated that most of the incorporated hydroxypropylcyclodextrins was released within about 30 min from the chitosan nanoparticles in pH 6.0 acetate buffer. In this work no significant burst of LC was observed during the initial hydrated stage.

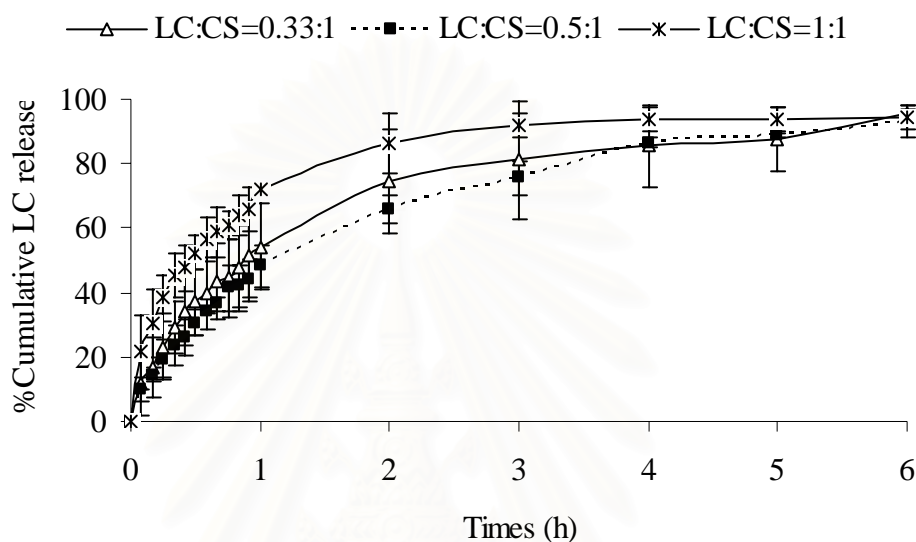


Figure 4.7 Comparison of %cumulative lidocaine release of CS-LC-Ps having different chitosan to drug ratios (Mw of CS=47 kDa; CS conc.= 0.25%CS). Error bars indicate the range of experimental reading obtained (sample number, $n = 3$).

SEM analysis was carried out to investigate the morphology of CS-LC-Ps after incubation for 6 h in phosphate buffer pH 7.4 (Figure 4.8). At 10,000 times magnification, two distinct feature of incubated particles were observed. One was that the particles was able to retain their integrity but with cracks all over the particle. The other feature was in the form of fibrous matrix. Since the fibrous matrix was not observed from the pre-incubated particles, it was therefore believed that this observation was a result of particle disintegration after the incubation in buffer. It must be added here that it has not yet known why some particles can hold their original shape but some cannot. Detailed analysis in this matter including change of CS molecular weight must be carried out in the future. In regard to the results obtained here, it is expected that the mechanism of drug release from the chitosan particles consists of

three steps: (i) swelling of particles; (ii) dissolution of lidocaine; and (iii) diffusion of lidocaine molecules through the cracks and disintegrated particles.

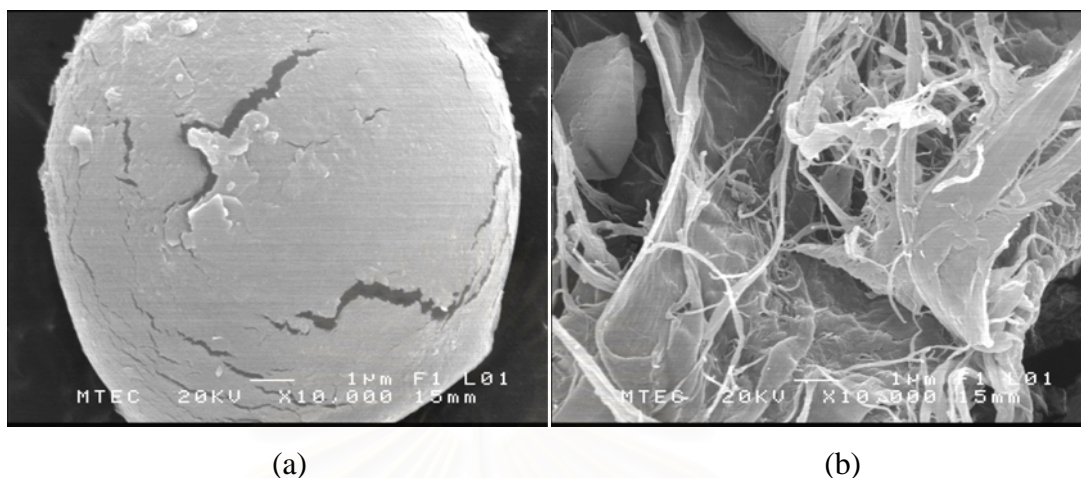


Figure 4.8 SEM of CS-LC-Ps (LC:CS mass ratio = 0.5:1) after incubation at 37°C for 6 h in phosphate buffer (pH = 7.4). The incubated particles either remained as particles with cracks (a) or disintegrate into fibrous matrix (b)

4.5 *In vitro* study of lidocaine permeation through membrane

4.5.1 Morphology and characteristic of membranes

General characteristics of shed snake skin specimens from *Naja kaouthia* are presented in Figure 4.9. The shed snake skin contains two different characteristic surfaces; scale and hinge (Figure 4.10-4.11).

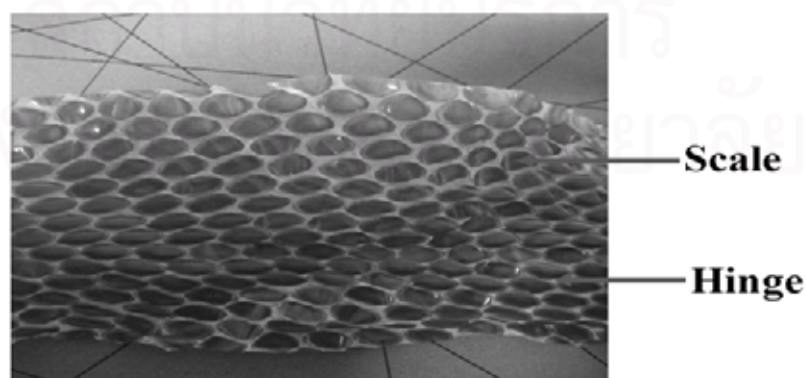


Figure 4.9 General characteristics of shed snake skin specimens from *Naja kaouthia*

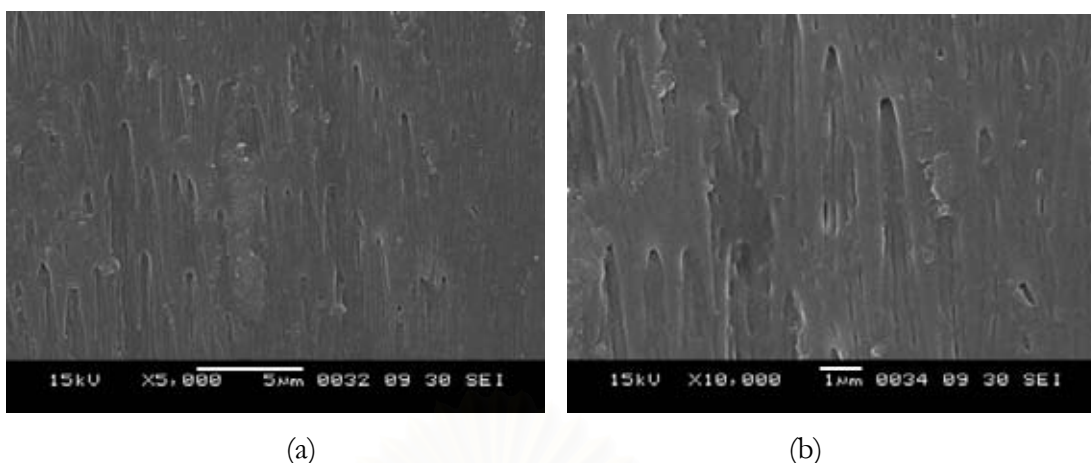


Figure 4.10 SEM of dorsal scale of shed snake skin specimens from *Naja kaouthia*; (a)×5,000 and (b)×10,000

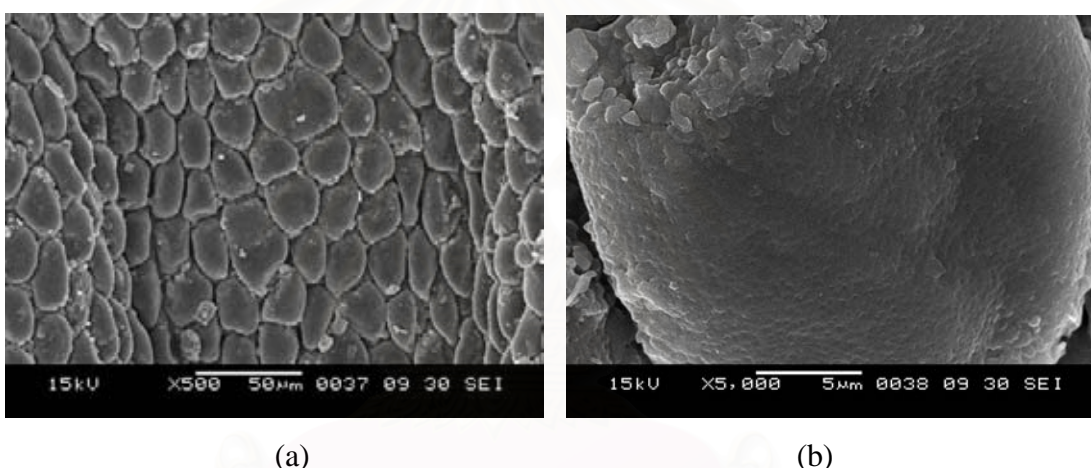


Figure 4.11 SEM of dorsal hinge of shed snake skin specimens from *Naja kaouthia*; (a)×5,000 and (b)×10,000

The thickness and lipid of the dorsal of shed snake skin are presented in Table 4.11. In this study, it was found that the thickness of shed snake skin is about 0.0471 mm. In addition, the purpose of using the shed snake skin is to use a model skin, which has similar lipid composition and permeability characteristics to those of human skin. It is well established that the lipid composition is an important factor regarding the barrier properties and permeability of skin [49]. The lipid content in the shed snake skin determined in this study was $26.80 \pm 7.23\%$, which was much different from that of human skin (2.0-6.5%), as reported by Opanasopit, P. et al. [50]. The reported lipid content in snakes by others in fact varied from 6% from *Elaphe obsoleta* [50] to 28% from *Elaphe obsoleta* [51]. It should be noted here that since LC is a small molecule

with superb solubility in water, the lipid content in snake skin should not significantly affect the penetration of the drug used in the Franz's cell setup used in this study.

The other membrane used in this study was cellulose membrane. Both shed snake skin and cellulose membrane had almost the same thickness as shown in Table 4.11. The cellulose membrane, however, did not contain any lipid.

Table 4.11 The thickness of shed snake skin and lipid within shed snake skin

Membrane	Thickness (mm)	Lipid (%)	Number of tests (n)
Shed snake skin	0.0471 ± 0.0024	26.80 ± 7.23	10
Cellulose membrane	0.0405 ± 0.0018	-	10

4.5.2 *In vitro* drug permeation through membranes

Shed snake skin membrane

In order to investigate the use of chitosan as a controlled release system for transdermal drug permeation, the percutaneous permeation of lidocaine as a model drug was evaluated in the form of CS-LC-Ps. In this study, LC:CS mass ratios were varied as 0.33:1, 0.5:1 and 1:1. All CS-LC-Ps were prepared from chitosan with MW of 47 kDa and %DD of 94. The chitosan concentration used to prepare the particles was 0.25% w/v. The *in vitro* permeation of lidocaine through the shed snake skin from CS-LC-Ps was calculated in terms of mean cumulative amount of permeated drug through a unit area of shed snake skin at each sampling time point for a total of 6 h (Figure 4.12). The results of lidocaine permeability through the shed snake skin are expressed as mean \pm standard deviation. Cumulative amounts of permeated drug through a unit area of shed snake skin ($\mu\text{g}/\text{cm}^2$) or Q_p in 6 hours showed the following trend: LC:CS mass ratio of 1:1 > 0.5:1 > 0.33:1. The Q_p values of 0.5:1 and 1:1 samples increased with time. This indicated that lidocaine was continuously released from the particles and permeated through the shed snake skin to accumulate in the buffer. On the other hand, the Q_p of lidocaine from pure LC, which was applied once on the shed snake skin, remained almost constant throughout 6 h. This suggested that the almost all LC permeated once

through the shed snake skin at the beginning of the experiment. In addition the amount of drug permeated was found to increase with increasing the lidocaine to chitosan mass ratio.

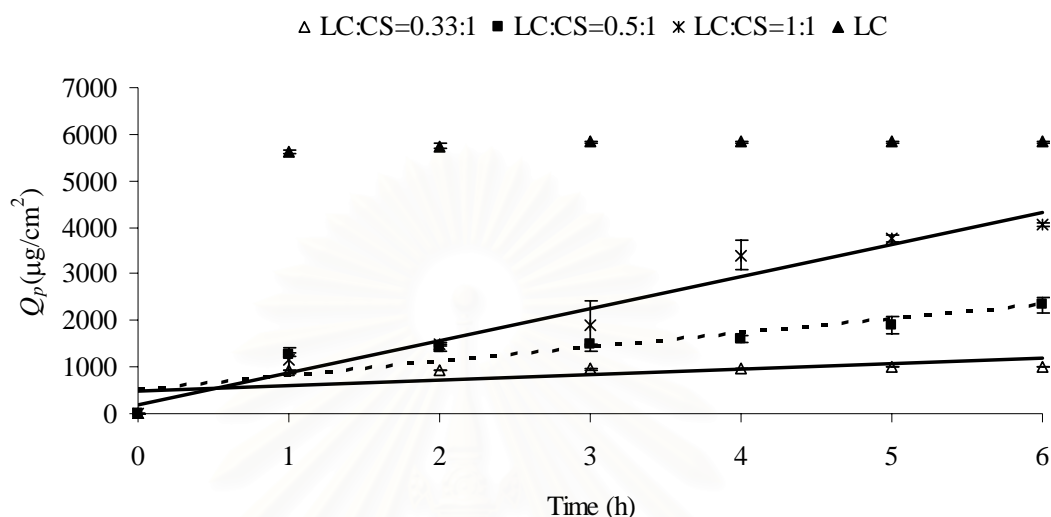


Figure 4.12 Permeation profiles of drug through shed snake skin (*Naja kaouthia*) at various lidocaine to chitosan mass ratios

Table 4.12 presents linear relationship between time and amount of drug permeating through shed snake skin (Q_p) as plotted in Figure 4.12. Permeation flux values of all sample sets were obtained from the slope of the plots. The permeation behaviors as determined from the relationship between time and Q_p were linear ($r^2 = 0.8146$ and 0.9617) for the samples with LC:CS of 0.5:1 and 1:1, while those of 0.33:1 and pure LC were not ($r^2 = 0.4600$ and 0.4027). The linear relationship between the amount of drug permeating through the membrane and time suggests that there is a continuous release of lidocaine from the chitosan particles, resulting in continuous drug permeation through the membrane in the 6 h period. Higher drug content in the chitosan particles therefore led to higher permeating flux ($302.4 \mu\text{g}/\text{cm}^2\cdot\text{h}$ for 0.5:1 and $690.4 \mu\text{g}/\text{cm}^2\cdot\text{h}$ for 1:1 CS-LC-Ps).

Table 4.12 Linear relationship between the amount of drug permeating through one area division of shed snake skin (Q_p) and time

Samples	Linear relationship	r^2	F ($\mu\text{g}/\text{cm}^2\cdot\text{h}$)
CS-LC-Ps (LC:CS = 0.33:1)	<i>Non linear relation</i>	0.4600	-
CS-LC-Ps (LC:CS = 0.5:1)	$Q_p = 302.4t + 518.21$	0.8146	302.4
CS-LC-Ps (LC:CS = 1:1)	$Q_p = 690.4t + 177.91$	0.9617	690.4
Pure LC	<i>Non linear relation</i>	0.4027	-

Cellulose membrane

The *in vitro* cellulose membrane permeation profiles of lidocaine are shown in Figure 4.13. In this study, LC:CS mass ratios were varied as 0.33:1, 0.5:1 and 1:1. All CS-LC-Ps were prepared from chitosan with Mw of 47 kDa and %DD of 94. The chitosan concentration used to prepare the particle was 0.25%w/v. The *in vitro* permeation of lidocaine through the cellulose membrane from CS-LC-Ps was calculated in terms of mean cumulative amount of permeated drug through a unit area of membrane (Q_p) at each sampling time point for a total of 6 h (Figure 4.12). In each sample, the Q_p within 6 h of incubation increased with time, indicating that lidocaine was continuously released from the particles and permeated through the cellulose membrane to accumulate in the buffer, the same behavior found from the shed snake skin. The relationship between time and amount of drug permeating through cellulose membrane (Q_p) (from the plot in Figure 4.13) as well as flux values are presented in Table 4.13. The permeation behaviors of all CS-LC-Ps (LC:CS = 0.33:1, 0.5:1, and 1:1) were found to be in linear relationship with time ($r^2 = 0.8837, 0.9188, \text{ and } 0.9337$). Similar to the case of snake skin, the linear relationship suggests that there is a continuous release of lidocaine from the chitosan particles, resulting in continuous drug permeation through the membrane in the 6 h period. Higher drug content in the chitosan particles therefore led to higher permeating flux ($278.5 \mu\text{g}/\text{cm}^2\cdot\text{h}$ for 0.33:1, $304.0 \mu\text{g}/\text{cm}^2\cdot\text{h}$ for 0.5:1, and $406.5 \mu\text{g}/\text{cm}^2\cdot\text{h}$ for 1:1 CS-LC-Ps).

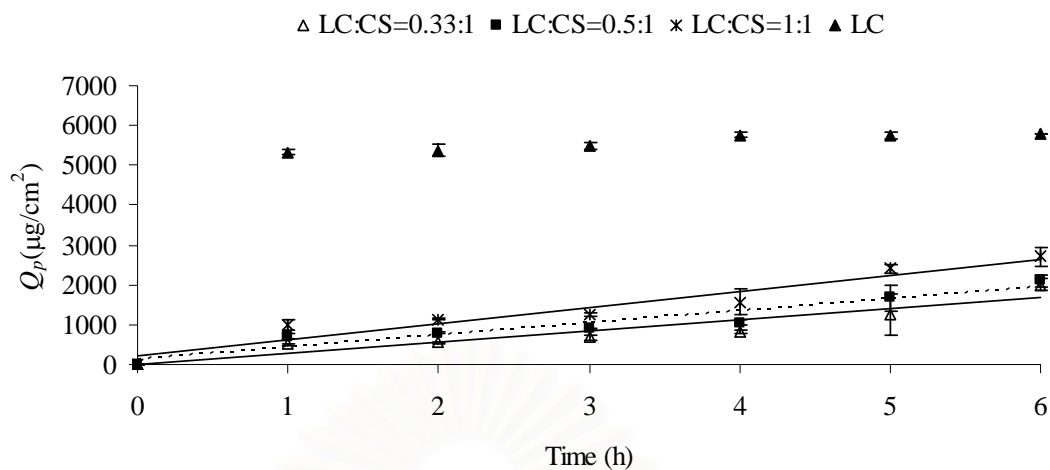


Figure 4.13 Permeation profiles of drug through cellulose membrane at various lidocaine to chitosan mass ratios

Table 4.13 Linear relationship between the amount of drug permeating through one area division of cellulose membrane (Q_p) and time

Samples	Linear relationship	r^2	F ($\mu\text{g}/\text{cm}^2 \cdot \text{h}$)
CS-LC-Ps (LC:CS = 0.33:1)	$Q_p = 278.5t - 3.4486$	0.8837	278.5
CS-LC-Ps (LC:CS = 0.5:1)	$Q_p = 304.0t + 120.73$	0.9188	304.0
CS-LC-Ps (LC:CS = 1:1)	$Q_p = 406.5t + 215.54$	0.9337	406.5
Pure LC	<i>Non linear relation</i>	0.4583	-

CHAPTER V

CONCLUSION AND SUGGESTIONS

5.1 Conclusion

Based on ultrasonic atomization technique, chitosan particles with sizes ranging from 250 to 1,520 nm were prepared from chitosan solution without any other coagulants or crosslinking agents. Lidocaine, a common local anesthetic, was used as a model drug and chitosan was used as supported polymer to prepare drug carrier in the form of particles with micro to nano sizes. The effects of molecular weight, degree of deacetylation, concentration of chitosan solution, and chitosan to lidocaine ratios on size and physicochemical properties were studied. Entrapment efficiency, drug release profile and drug permeation of lidocaine in the prepared chitosan particles were also investigated.

The averaged dry particle size tended to increase but not statistically significant when the molecular weights increased from 47 to 238 kDa. But in the hydrated state the particle sizes increased significantly from 553 ± 96 to $1,041\pm 156$ nm with increasing the MW from 75 to 238 kDa. In order to get small CS particle size, CS with high DD and low CS concentration should be used. Increasing the lidocaine content tended to significantly increase the size of dry particles but not the hydrated particles.

Increasing in hydrogen bonding between chitosan and lidocaine was observed by IR analysis since both compounds possessed similar amine and amide functional groups. X-ray analysis of the lidocaine-filled CS particles did not reveal any crystallized domain in the prepared particles. The lidocaine content within CS-LC-Ps was increased with the increasing chitosan to drug ratio but decreased with chitosan molecular weight increased.. The entrapment efficiency of 90% could be successfully achieved.

Lidocaine release from chitosan particles was studied in phosphate buffer medium at 37°C indicating that up to 92% of lidocaine was released from the particles within the period of 3 hours with no significant burst of drug during the initial hydrated stage. A simulated skin permeation study of the lidocaine-filled chitosan particles was also carried out by using shed snake skin and cellulose membrane. Lidocaine was continually released from the particles for up to 6 hours of study.

5.2 Suggestions

From this study, it can be seen that particles with less than 100 nm in size has not yet achieved. The particle preparation method should be tested by using chitosan with molecular weight lower than 47 kDa that was used in this study. Care must be taken in terms of particle stability because the particle tends to disintegrate when low molecular weight polymer is used. In addition, as already mentioned in Chapter 4, the particle degradation behavior should be studied in detail, especially the changes in molecular weight of chitosan after incubation for a certain period in PBS buffer. Finally a study for large scale preparation of the particles is also needed, since it was found in this study that the process required a long operation time to obtain a small amount of particles (0.36 g per h).

REFERENCES

- [1] Ramanathan, S., and Block, L.H. The use of chitosan gels as matrices for electrically-modulated drug delivery. Journal of Controlled Release 70 (2001): 109-123.
- [2] Asada, M., Takahashi, H., Okamoto, H., Tanino H., and Danjo K. Theophylline particle design using chitosan by the spray drying. International Journal of Pharmaceutics 270(2004): 167–174.
- [3] Agnihotri, S. A., Mallikarjuna, N. N., and Aminabhavi, T. M. Recent advances on chitosan-based micro-and nanoparticles in drug delivery. Journal of Controlled Release 100(2004): 5-28.
- [4] Tang, E.S.K., Huang, M., and Lim, L.Y. Ultrasonication of chitosan and chitosan nanoparticles. International Journal of Pharmaceutics 265(2003): 103-114.
- [5] Boonsongrit, Y., Mitrevej, A., and Mueller, B. W. Chitosan drug binding by ionic interaction. European Journal of Pharmaceutics and Biopharmaceutics 62 (2006): 267-274.
- [6] Tiyaboonchai, W. Preparation and evaluation of chitosan carbosymethyl cellulose sustained microcapsules containing indomethacin. Major Manufacturing Pharmacy, Faculty of pharmacy, Chulalongkorn University, 1994.
- [7] Kumar, M.N.V.R. A review of chitin and chitosan applications. Reactive & Functional Polymers 46(2000): 1-27.

- [8] Robert, G.A.F. 1994. Structure-properties relationship in chitin and its derivatives. Proceeding from Asia-Pacific Chitin and Chitosan Symposium. Bangi, Malaysia, np.
- [9] Muzzarelli, RAA. 1977. Chitin. Oxford, Pergamon Press, 326 p.
- [10] Material Safety Data Sheet; Lidocaine Hydrochloride monohydrate MSDS
Available from: [http://www.sciencelab.com/xMSDS-Lidocaine Hydrochloride monohydrate-9924493](http://www.sciencelab.com/xMSDS-Lidocaine-Hydrochloride-monohydrate-9924493).
- [11] Broadhead, J., Rouan, S. K. E., Hau, I., and Rhodes, C T. The effect of process an formulation variables on the properties of spray-dried β -galactosidase. Journal of Pharmacy and Pharmacology 46(1994): 458-467.
- [12] Corrigan, O. I., and Holohan, E. M. Amorphous spray-dried hydroflumethiazide polyvinylpyrrolidone system physicochemical properties. Journal of Pharmaceutics Pharmacological 36(1984): 217-226.
- [13] Tsuda, Y., Ischida, M., Suzuki, E., and Sekiguchi, K. Spray drying of grise of ulvin solution forming its solvate. Chemical and Pharmaceutical Bulletin. 36(6)(1988): 2193-2196.
- [14] Wan, L.S.C., Heng, P.W.S., and Chia, C.G.H. 1990. Influence of operational and formulation factors on spray dried microcapsules. JSPS-NUS Seminar on "Recent developments in pharmaceutical technology", pp. 190-206. Japan:Chiba.
- [15] Broadhead, J., Edmond-Rouan, S.K., and Rhodes, C.T. The spray drying of Pharmaceuticals. Drug Development and Industrial Pharmacy 18(1992): 1169-1206.

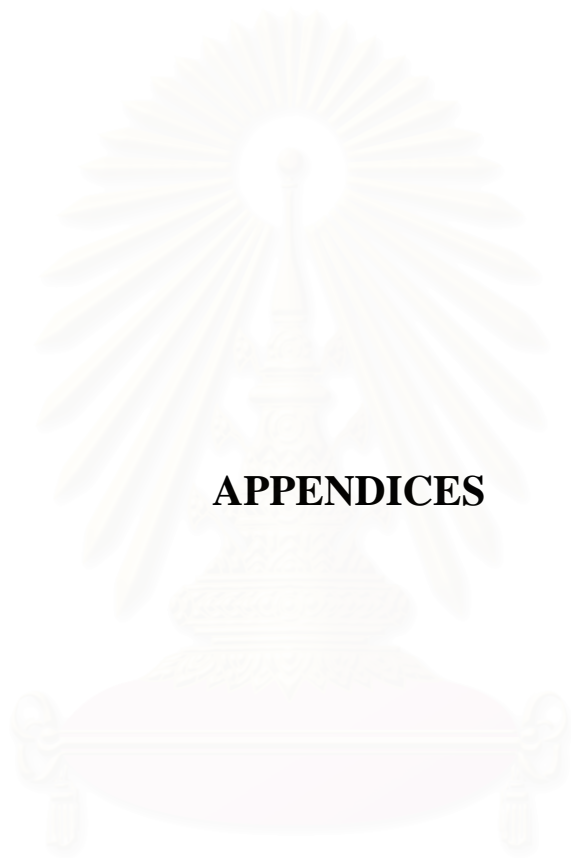
- [16] Master, K. 1979. Spray drying handbook (3 rd. ed.). New York: John Wiley&Sons.
- [17] Agnihotri, S.A., Mallikarjuna, N.N., and Aminabhavi. T.M. Recent advances on chitosan-based micro- and nanoparticles in drug delivery. Journal of Controlled Release 100(2004): 5-28.
- [18] Lorenzo-Lamosa, M.L., Remunan-Lopez , C., Vila-Jato, J.L., and M.J. Alons Design of microencapsulated chitosan microspheres for colonic drug delivery. Journal of Controlled Release 52(1998): 109-118.
- [19] Polakovic, M., Gorner, T., Gref, R., and Dellacherie, E. Lidocaine loaded biodegradable nanospheres II. Modelling of drug release. Journal of Controlled Release 60(1999): 169–177.
- [20] Mao, H.Q., Roy, K., Troung-Le, V.L., Janes, K.A., Lim, K.Y., Wang, Y., August, J.T., and Leong, K.W. Chitosan DNA nanoparticles as gene delivery carriers: synthesis, characterization and transfection efficiency, Journal of Controlled Release 70(2001): 399-421.
- [21] Mitra, S., Gaur, U., Ghosh, P.C., and Maitra, A.N. Tumor targeted delivery of encapsulated dextran-doxorubicin conjugate using chitosan nanoparticles as carrier. Journal of Controlled Release 74(2001): 317-323.
- [22] Kumbar, S.G., Kulkarni, A.R., and Aminabhavi, T.M. Cross-linked chitosan micro spheres for encapsulation of diclofenac sodium: effect of cross-linking agent. Journal of Microencapsulation 19(2002): 173-180.
- [23] Hua, Y., Jianga, X., Dinga, Y., Gea, H., Yuanb, Y., and Yang, C. Synthesis and characterization of chitosan-poly(acrylic acid) nanoparticles. Biomaterials 23 (2002): 3193-3201.

- [24] Pan, Y., Li, Y., Zhao, H., Zheng, J., Xu, H., Wei, G., Hao, J., and Cui, F.
Chitosan nanoparticles improve the intestinal absorption of insulin *in vivo*.
International Journal of Pharmaceutics 249(2002): 139-147.
- [25] Grenha, A., Seijo, B., and Remunan-Lopez, C. Microencapsulated chitosan
nanoparticles for lung protein delivery. European Journal of
Pharmaceutical Sciences 25(2005): 427-437.
- [26] Schmitz, T., Bravo-Osuna, I., Vauthier, C., Ponchel, G., Loretz, B., and
Bernkop-Schnurch, A. Development and *in vitro* evaluation of a thiomers-
based nanoparticulate gene delivery system. Journal of Biomaterials
28(2007): 524-531.
- [27] Baldwin, S.P., and Saltzman, W.M. Materials for protein delivery in tissue
engineering. Advanced Drug Delivery Reviews 33(1998): 71-86.
- [28] Lisa Brannon-Peppas. Biomaterials: Polymers in Controlled Drug Delivery.
Available from: <http://www.devicelink.com/mpb/archive/97/11/003.html>
[1997]
- [29] Advances in Controlled Release Technology: Polymeric Delivery Systems for
Pharmaceuticals, Proteins and Other Agents. Available from:
http://web.mit.edu/mitpep/pi/courses/controlled_release_technology.html
[2008, July 21-25]
- [30] Bosman, Ingrid J., Ensing, K., and Zeeuw, Rokus A. de. Standardization
procedure for the *in vitro* skin permeation of anticholinergics.
International Journal of Pharmaceutics 169(1998): 65-73.
- [31] Perme Gear, Inc. Equipment that measures permeation through membranes.
Available from: <http://www.permegear.com/fc01.gif> [2005]

- [32] Modamio, P., Lastra, C. F., and E. L. Marino. A comparative *in vitro* study of percutaneous penetration of blockers in human skin. International Journal of Pharmaceutics 194(2000): 249-259.
- [33] Modamio, P., Lastra C. F., and Marino, E. L. Transdermal absorption of celiprolol and bisoprolol in human skin *in vivo*. International Journal of Pharmaceutics 173(1998): 141-148.
- [34] Minghetti, P., Casiraghi, A., Montanari, L., and Monzani M.V. *In vitro* skin permeation of sinitrodil, a member of a new class of nitrovasodilator drugs. European Journal of Pharmaceutical Sciences 7(1999): 231-236.
- [35] Puglia, C., Bonina, F., Trapani, G., Franco, M., and Ricci, M. Evaluation of *in vitro* percutaneous absorption of lorazepam and clonazepam from hydro-alcoholic gel formulations. International Journal of Pharmaceutics 228(2001): 79-87.
- [36] Paula, C., Gareth, W., and Charles, M. H. Triclosan: release from transdermal adhesive formulations and *in vitro* permeation across human epidermal membranes. International Journal of Pharmaceutics 235(2002): 229-236.
- [37] Magnoson, B. M., and Koskinen, L.O.D. *In vitro* percutaneous penetration of topically applied capsaicin in relation to *in vivo* sensation responses. International Journal of Pharmaceutics 195(2000): 55-62.
- [38] Sartorelli, P., Andersen, H. R., Angerer, J., Corish, J., Drexler, H., Goen, T., Griffin, P., Hotchkiss, S. A. M., Larese, F., Montomoli, L., Perkins, J., Schmelz, M., Sandt, J. van de, and Williams, F. Percutaneous penetration studies for risk assessment. Environment Toxicology and Pharmacology 8 (2002): 133-152.

- [39] Kimura, C., Nakanishi, T., and Tojo K. Skin permeation of ketotifen applied from stick-type formulation. European Journal of Pharmaceutics and Biopharmaceutics 67(2007): 420-424.
- [40] Xie, Y., Xu, B., PhD, and Gao, Y. Controlled transdermal delivery of model drug compounds by MEMS microneedle array. Nanomedicine: Nanotechnology, Biology, and Medicine 1(2005): 184-190.
- [41] Ropke, C.D., Kaneko, T.M., Rodrigues, R.M., Silva, V.V. da, Barros, S., Sawada, Tania C. H., Kato, Massuo J., and Barros, Silvia B. M. Evaluation of percutaneous absorption of 4-nerolidylcatechol from four topical formulations. International Journal of Pharmaceutics 249(2002): 106-116.
- [42] Bowen, Jenna L., and Heard, Charles M. Film drying and complexation effects in the simultaneous skin permeation of ketoprofen and propylene glycol from simple gel formulations. International Journal of Pharmaceutics 307(2006): 251-257.
- [43] Kerec, M., Bogataj, M., Veranic, P., and Mrhar, A. Permeability of pig urinary bladder wall: the effect of chitosan and the role of calcium. European Journal of Pharmaceutical Sciences 25(2005): 113-121.
- [44] Ngawhirunpat, T., Opanasopit, P., and Prakongpan, S. Comparison of skin transport and metabolism of ethyl nicotinate in various species. Journal of Pharmaceutics and Biopharmaceutics 58(2004): 645-651.
- [45] Kang, L., Jun, H.W., and McCall, J.W. Physicochemical studies of lidocaine-menthol binary systems for enhanced membrane transport. International Journal of Pharmaceutics 206(2000): 35-42.

- [46] Muzzarelli, RAA, and Rocchetti, R. Determination of the degree of acetylation of chitosans by first derivative ultraviolet spectrophotometry. Carbohydrate Polymers 5(1985): 461-72.
- [47] McILVAINE, T. C. A buffer solution for colorimetric comparison. The Journal of Biological Chemistry (1921): 183-186.
- [48] Maestrelli, F., Garcia-Fuentes, M., Mura, P., Jose Alonso, M. A new drug nanocarrier consisting of chitosan and hydroxypropylcyclodextrin. European Journal of Pharmaceutics and Biopharmaceutics 63(2006): 79-86.
- [49] Asbill, C., Kim, N., El-Kattan, A., Creek, K., Wertz, P., and Michniak, B. Evaluation of a Human Bio-Engineered Skin Equivalent for Drug Permeation Studies. Pharmaceutical Research 2000: 1092-1097.
- [50] Opanasopit, P., Shiraishi, K., Nishikawa, M., Yamashita, F., Takakura, Y., and Hashida M. 1999. Lectin-dependent biodistribution of glycosylated drug carriers targeted to liver nonparenchymal cells. ODD Japanese Pharmaceutical sciences conference 14 th, March 26-28, 1999. Ogayama, Japan.
- [51] Panomsuk, S., Ngawhlrunpat, T., and Opanasopit, P. Skin permeation of drugs: using shed snake skin as a model membrane. Department of Pharmaceutical Technology, Faculty of Pharmacy, Silpakorn University, 2002.



APPENDICES

สถาบันวิทยบริการ
จุฬาลงกรณ์มหาวิทยาลัย

Appendix A

Statistic analysis

In case of particle size as measured by SEM

Table 1A Effect of molecular weight on particle size of CS-Ps

Mw (kDa)	DD (%)	CS conc. (% w/v)	Mean size (nm)	Variance	N
75	94	0.5	556.34	63516.9539	100
150	90	0.5	563.10	49241.2626	100
238	95	0.5	607.09	29095.2746	100

P = 0.2024234

At the 0.05 level,

the three means are no significantly different.

47	94	0.25	432.46	30897.4428	100
75	94	0.25	464.86	39484.364	100
150	90	0.25	465.48	66910.8784	100

P = 0.4595593

At the 0.05 level,

the three means are no significantly different.

Table 2A Effect of %DD on particle size of CS-Ps

Mw (kDa)	DD (%)	CS conc. (% w/v)	Mean size (nm)	Variance	N
150	76	0.5	619.09	83906.3656	100
150	82	0.5	578.03	102602.878	100
150	90	0.5	563.10	49241.2626	100

$P = 0.344425$

At the 0.05 level,

the three means are no significantly different.

Table 3A Effect of chitosan concentration on particle size of CS-Ps

Mw (kDa)	DD (%)	CS conc. (% w/v)	Mean size (nm)	Variance	N
75	94	0.25	464.86	39484.364	100
75	94	0.50	556.34	63516.9539	100
75	94	0.75	595.28	57305.739	100
75	94	1.50	798.42	173270.852	100

$P = 3.572 \times 10^{-14}$

At the 0.05 level,

the four means are significantly different.

Table 4A Effect of lidocaine to chitosan mass ratio on particle size of CS-LC-Ps

Mw (kDa)	DD (%)	CS conc. (% w/v)	Ratio of LC:CS (w/w)	Mean size (nm)	Variance	N
75	94	0.5	0.33:1	499.30	53297.303	100
75	94	0.5	0.5:1	663.13	144878.316	100
75	94	0.5	1:1	679.03	103287.262	100

$$P = 7.204 \times 10^{-5}$$

At the 0.05 level,

the three means are significantly different.

47	94	0.25	0.33:1	442.10	24474.3737	100
47	94	0.25	0.5:1	485.56	76874.2489	100
47	94	0.25	1:1	669.33	245144.021	100

$$P = 5.61 \times 10^{-6}$$

At the 0.05 level,

the three means are significantly different.

Table 5A Effect of chitosan molecular weight on particle size of CS-LC-Ps

Mw (kDa)	DD (%)	CS conc. (% w/v)	Ratio of LC:CS (w/w)	Mean size (nm)	Variance	N
47	94	0.25	0.5:1	485.56	76874.2489	100
75	94	0.25	0.5:1	525.04	67964.6448	100
150	90	0.25	0.5:1	709.27	111951.027	100

$$P = 1.392 \times 10^{-7}$$

At the 0.05 level,

the three means are significantly different.

In case of particle size as measured by particle sizer

Table 6A Effect of molecular weight on particle size of CS-Ps

Mw (kDa)	DD (%)	CS conc. (%w/v)	Mean size (nm)	Variance	N
75	94	0.5	553.3333333	9216.3333	3
150	90	0.5	876.6666667	11704.333	3
238	95	0.5	1041	24193	3

P = 0.00756634

At the 0.05 level,
the three means are significantly different.

47	94	0.25	250.3333333	134.33333	3
75	94	0.25	417	1521	3
150	90	0.25	530	55069	3

P = 0.11661695

At the 0.05 level,
the three means are no significantly different.

Table 7A Effect of %DD on particle size of CS-Ps

Mw (kDa)	DD (%)	CS conc. (%w/v)	Mean size (nm)	Variance	N
150	76	0.5	876.6666667	11704.333	3
150	82	0.5	903	7147	3
150	90	0.5	1136.666667	14933.333	3

P = 0.04464962

At the 0.05 level,
the three means are significantly different.

Table 8A Effect of chitosan concentration on particle size of CS-Ps

Mw (kDa)	DD (%)	CS conc. (% w/v)	Mean size (nm)	Variance	N
75	94	0.25	417	1521	3
75	94	0.50	553.3333333	9216.3333	3
75	94	0.75	998.6666667	10745.333	3
75	94	1.50	1520	2800	3

$$P = 5.004 \times 10^{-7}$$

At the 0.05 level,
the four means are significantly different.

Table 9A Effect of chitosan to drug ratio on particle size of CS-LC-Ps

Mw (kDa)	DD (%)	CS conc. (% w/v)	Ratio of LC:CS (w/w)	Mean size (nm)	Variance	N
75	94	0.5	0.33:1	1024.666667	35365.333	3
75	94	0.5	0.5:1	1131.333333	26945.333	3
75	94	0.5	1:1	1301.333333	79865.333	3

$$P = 0.35609822$$

At the 0.05 level,
the three means are no significantly different.

47	94	0.25	0.33:1	706.3333333	6066.333333	3
47	94	0.25	0.5:1	708.3333333	17030.33333	3
47	94	0.25	1:1	883.3333333	13604.33333	3

$$P = 0.15946032$$

At the 0.05 level,
the three means are significantly different.

Table 10A Effect of chitosan molecular weight on particle size of CS-LC-Ps

Mw (kDa)	DD (%)	CS conc. (% w/v)	Ratio of LC:CS (w/w)	Mean size (nm)	Variance	N
47	94	0.25	0.5:1	708.3333333	17030.333	3
75	94	0.25	0.5:1	771	4951	3
150	90	0.25	0.5:1	776.6666667	11374.333	3

$P = 0.69425979$

At the 0.05 level,

the three means are no significantly different.

สถาบันวิทยบริการ
จุฬาลงกรณ์มหาวิทยาลัย

Appendix B

Calibration Curve

The concentration versus absorbance of lidocaine in distilled water at 262 nm. and in phosphate buffer pH 7.4 at 262 nm. are presented in Table 1 and 2 showing a linear relationship with the correlation coefficient = 0.9996 and 0.9988

Table 1B Absorbance of lidocaine in distilled water determined at 262 nm.

Concentration of lidocaine in distilled water ($\times 10^{-5}$ g/mL)	Absorbance
8	0.13666
9	0.14380
10	0.15474
20	0.31094
30	0.46736
40	0.62253

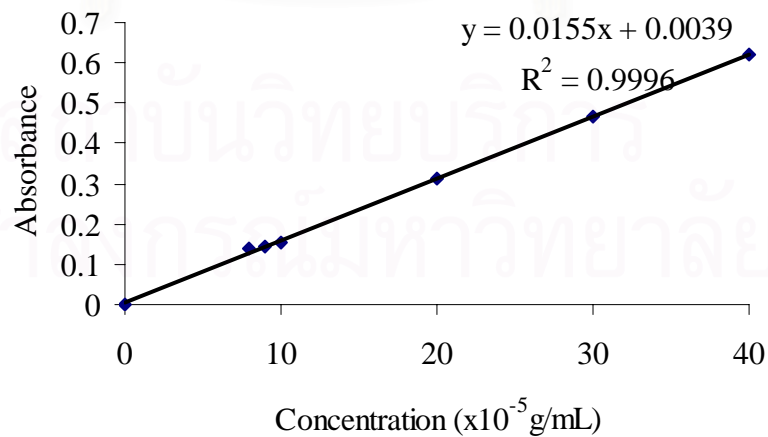


Figure 1B Standard calibration curve of absorbance of lidocaine in distilled water

$$\text{Concentration of lidocaine solution} = \frac{A - 0.0039}{0.0155 \times 10} \text{ g/mL}$$

$$\begin{aligned} \text{Amount of lidocaine (g/g of CS - LC NPs)} \\ = \frac{\text{Concentration of lidocaine (g/mL)}}{0.025 \text{ g}} \times 100 \text{ mL} \end{aligned}$$

Table 2B Absorbance of lidocaine in phosphate buffer solution pH 7.4 determined at 262 nm.

Concentration of lidocaine in phosphate buffer solution pH 7.4 ($\times 10^{-5}$ g/mL)	Absorbance
10	0.080876
20	0.15902
30	0.22751
40	0.29704
50	0.35767
60	0.42935
70	0.50564

$$\text{Concentration of lidocaine solution} = \frac{A - 0.0093}{0.071 \times 10} \text{ g/mL}$$

$$\begin{aligned} \text{Amount of lidocaine release (g/g of CS - LC - Ps)} \\ = \frac{\text{Concentration of lidocaine (g/mL)}}{0.25 \text{ g}} \times 500 \text{ mL} \end{aligned}$$

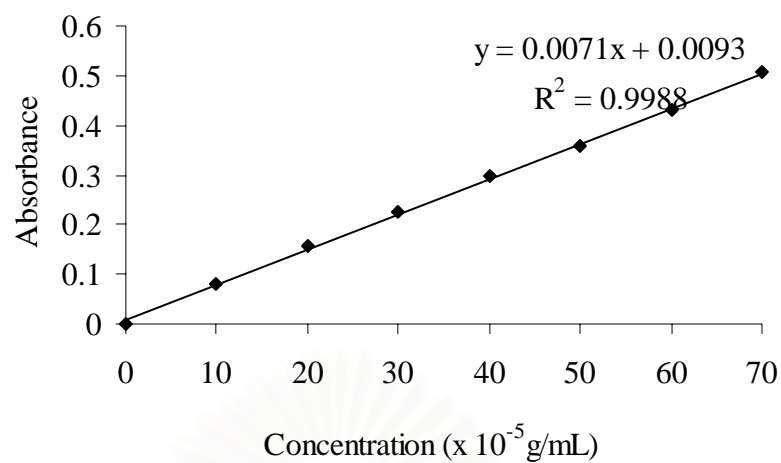


Figure 2B Standard calibration curve of absorbancy of lidocaine in phosphate buffer solution pH 7.4

Appendix C

Amount of Drug Release

Table 1C Cumulative LC release from CS-LC-Ps for case of LC:CS mass ratio = 0.33:1

Time (min)	Amount of LC release (g/g of CS-LC NPs)				
	1	2	3	Mean	SD
0	0	0	0	0	0
5	0.01485	0.0117	0.0515	0.0260	0.0221
10	0.0269	0.0238	0.0625	0.0377	0.0215
15	0.0365	0.0417	0.0784	0.0522	0.0228
20	0.0572	0.0528	0.0863	0.0654	0.0182
25	0.0604	0.0663	0.1054	0.0774	0.0245
30	0.0655	0.0751	0.1101	0.0836	0.0235
35	0.0687	0.0831	0.118	0.0899	0.0254
40	0.0745	0.0934	0.1261	0.0980	0.0261
45	0.0752	0.0972	0.1296	0.1007	0.0274
50	0.0784	0.1045	0.1388	0.1072	0.0303
55	0.0823	0.1213	0.1435	0.1157	0.0310
60	0.0879	0.1336	0.1455	0.1223	0.0304
120	0.1319	0.1673	0.2049	0.1680	0.0365
180	0.1350	0.2047	0.209	0.1829	0.0415
240	0.1603	0.2049	0.2128	0.1923	0.0283
300	0.1715	0.2069	0.2139	0.1974	0.0227
360	0.2165	0.2131	0.2173	0.2156	0.0022

Table 2C Cumulative LC release from CS-LC-Ps for case of LC:CS mass ratio = 0.5:1

Time (min)	Amount of LC release (g/g of CS-LC NPs)				
	1	2	3	Mean	SD
0	0	0	0	0	0
5	0.0413	0.0314	0.0181	0.0303	0.0116
10	0.0511	0.0402	0.0402	0.0438	0.0063
15	0.0733	0.0403	0.0631	0.0589	0.0169
20	0.077	0.0501	0.0863	0.0711	0.0188
25	0.0835	0.06	0.0929	0.0788	0.0169
30	0.0993	0.078	0.0992	0.0922	0.0123
35	0.1021	0.1006	0.1036	0.1021	0.0015
40	0.1042	0.1066	0.1176	0.1095	0.0071
45	0.1048	0.1203	0.1485	0.1245	0.0222
50	0.1092	0.1223	0.1487	0.1267	0.0201
55	0.1252	0.1225	0.1532	0.1336	0.017
60	0.1448	0.1254	0.1657	0.1453	0.0202
120	0.1877	0.2133	0.1932	0.1981	0.0135
180	0.2097	0.2394	0.2348	0.228	0.016
240	0.2643	0.2617	0.256	0.2607	0.0042
300	0.2663	0.2692	0.2671	0.2675	0.0015
360	0.2753	0.2693	0.2977	0.2808	0.015

Table 3C Cumulative LC release from CS-LC-Ps for case of LC:CS mass ratio = 1:1

Time (min)	Amount of LC release (g/g of CS-LC NPs)				
	1	2	3	Mean	SD
0	0	0	0	0	0
5	0.1179	0.0712	0.0367	0.0753	0.0408
10	0.1445	0.1049	0.0714	0.1069	0.0366
15	0.1626	0.126	0.1153	0.1346	0.0248
20	0.1824	0.1353	0.157	0.1582	0.0236
25	0.194	0.1439	0.1635	0.1671	0.0252
30	0.2037	0.1675	0.1793	0.1835	0.0185
35	0.2213	0.1736	0.1986	0.1978	0.0239
40	0.2251	0.1755	0.2179	0.2062	0.0268
45	0.2265	0.1964	0.2186	0.2138	0.0156
50	0.2389	0.1993	0.2329	0.2237	0.0213
55	0.2465	0.2042	0.2414	0.2307	0.0231
60	0.2554	0.2446	0.2569	0.2523	0.0067
120	0.3193	0.2646	0.3236	0.3025	0.0329
180	0.3367	0.3085	0.3213	0.3222	0.0141
240	0.3389	0.3133	0.3324	0.3282	0.0133
300	0.339	0.3139	0.3341	0.329	0.0133
360	0.3419	0.3153	0.3346	0.3306	0.0137

Appendix D

Percentage of Cumulative Drug Release

Table 1D Percentage of LC release from CS-LC-Ps for case of LC:CS mass ratio = 0.33:1

Time (min)	Percentage of LC Release				
	1	2	3	Mean	SD
0	0	0	0	0	0
5	6.59	5.19	22.84	11.54	9.81
10	11.93	10.55	27.72	16.73	9.54
15	16.19	18.49	34.77	23.15	10.13
20	25.37	23.41	38.27	29.02	8.07
25	26.78	29.4	46.74	34.31	10.85
30	29.05	33.3	48.82	37.06	10.41
35	30.47	36.85	52.33	39.88	11.24
40	33.04	41.42	55.92	43.46	11.58
45	33.35	43.1	57.47	44.64	12.13
50	34.77	46.34	61.55	47.55	13.43
55	36.5	53.79	63.64	51.31	13.74
60	38.98	59.25	64.52	54.25	13.48
120	58.49	74.19	90.86	74.51	16.19
180	59.87	90.78	92.68	81.11	18.42
240	71.09	90.86	94.37	85.44	12.55
300	76.05	91.75	94.86	87.55	10.08
360	96.01	94.5	96.36	95.62	0.99

Table 2D Percentage of LC release from CS-LC-Ps for case of LC:CS mass ratio = 0.5:1

Time (min)	Percentage of LC Release				
	1	2	3	Mean	SD
0	0	0	0	0	0
5	13.71	10.42	6.01	10.05	3.86
10	16.97	13.35	13.35	14.56	2.09
15	24.34	13.38	20.95	19.56	5.61
20	25.56	16.63	28.65	23.61	6.24
25	27.72	19.92	30.84	26.16	5.62
30	32.97	25.9	32.93	30.6	4.07
35	33.9	33.4	34.4	33.9	0.5
40	34.59	35.39	39.04	36.34	2.37
45	34.79	39.94	49.3	41.34	7.36
50	36.25	40.6	49.37	42.07	6.68
55	41.57	40.67	50.86	44.37	5.64
60	48.07	41.63	55.01	48.24	6.69
120	62.32	70.82	64.14	65.76	4.48
180	69.62	79.48	77.95	75.68	5.31
240	87.75	86.89	84.99	86.54	1.41
300	88.41	89.38	88.68	88.82	0.5
360	91.4	89.41	98.84	93.22	4.97

Table 3D Percentage of LC release from CS-LC-Ps for case of LC:CS mass ratio =1:1

Time (min)	Percentage of LC Release				
	1	2	3	Mean	SD
0	0	0	0	0	0
5	33.64	20.31	10.47	21.47	11.63
10	41.23	29.93	20.37	30.51	10.44
15	46.39	35.95	32.9	38.41	7.07
20	52.04	38.6	44.79	45.14	6.73
25	55.35	41.06	46.65	47.69	7.2
30	58.12	47.79	51.16	52.36	5.27
35	63.14	49.53	56.66	56.44	6.81
40	64.22	50.07	62.17	58.82	7.65
45	64.62	56.03	62.37	61.01	4.45
50	68.16	56.86	66.45	63.82	6.09
55	70.33	58.26	68.87	65.82	6.59
60	72.87	69.79	73.3	71.99	1.91
120	91.1	75.49	92.33	86.31	9.39
180	96.06	88.02	91.67	91.92	4.03
240	96.69	89.39	94.84	93.64	3.8
300	96.72	89.56	95.32	93.87	3.79
360	97.55	89.96	95.46	94.32	3.92

Appendix E

In Vitro Skin Permeation

Table 1E Cumulative amount of permeated drug through a unit area of shed snake skin (Q_p), $\mu\text{g}/\text{cm}^2$ for case of LC:CS mass ratio = 0.33:1

Time (hour)	Q_p (1)	Q_p (2)	Q_p (3)	Mean	SD
0	0	0	0	0	0
1	927.38	927.57	929.77	928.24	1.33
2	935.11	938.65	943.33	939.03	4.12
3	948.96	950.30	952.31	950.52	1.69
4	969.78	972.45	975.79	972.67	3.01
5	997.76	998.14	1003.29	999.73	3.09
6	1016.85	1017.43	1017.71	1017.30	0.44

Table 2E Cumulative amount of permeated drug through a unit area of shed snake skin (Q_p), $\mu\text{g}/\text{cm}^2$ for case of LC:CS mass ratio = 0.5:1

Time (hour)	Q_p (1)	Q_p (2)	Q_p (3)	Mean	SD
0	0	0	0	0	0
1	1218.43	1257.2	1322.89	1266.20	52.81
2	1338.65	1411.32	1457.34	1402.40	59.84
3	1461.83	1478.45	1495.92	1478.70	17.05
4	1532.01	1572.5	1685.18	1596.60	79.37
5	1786.87	1807.02	2098.93	1897.60	174.64
6	2143.81	2427.41	2439.92	2337.00	167.46

Table 3E Cumulative amount of permeated drug through a unit area of shed snake skin (Q_p), $\mu\text{g}/\text{cm}^2$ for case of LC:CS mass ratio = 1:1

Time (hour)	Q_p (1)	Q_p (2)	Q_p (3)	Mean	SD
0	0	0	0	0	0
1	963.57	993.94	1451.9	1136.5	273.59
2	1468.89	1504.03	1521.12	1498	26.63
3	1542.71	1611.17	2514.87	1889.6	542.59
4	3061.16	3464.98	3665.69	3397.3	307.9
5	3698.16	3739.32	3850.18	3762.6	78.63
6	4014.32	4052.52	4113.15	4060	49.84

Table 4E Cumulative amount of permeated drug through a unit area of shed snake skin (Q_p), $\mu\text{g}/\text{cm}^2$ for case of LC

Time (hour)	Q_p (1)	Q_p (2)	Q_p (3)	Mean	SD
0	0	0	0	0	0
1	5565.49	5661.24	5625.28	5617.3	48.36
2	5723.86	5826.12	5706.55	5752.2	64.62
3	5829.79	5826.72	5828.68	5828.4	1.55
4	5829.86	5825.82	5828.58	5828.1	2.06
5	5829.84	5825.93	5828.69	5828.2	2.01
6	5829.38	5825.94	5828.7	5828	1.82

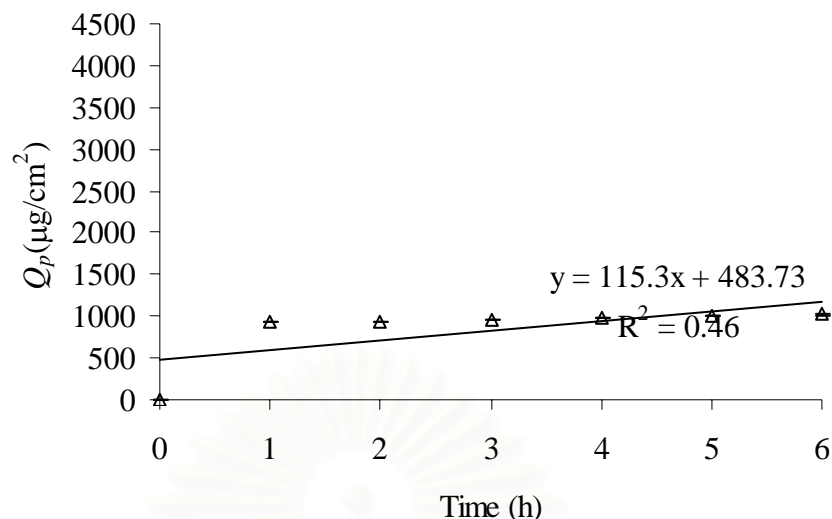


Figure 1E Permeation profiles of drug through shed snake skin (*Naja kaouthia*) for case of CS-LC-Ps (LC:CS mass ratio = 0.33:1). Q_p =Cumulative amount of permeated drug through a unit area of shed snake skin, $\mu\text{g}/\text{cm}^2$, t =time (h). Each data represents the mean \pm SD (n=3).

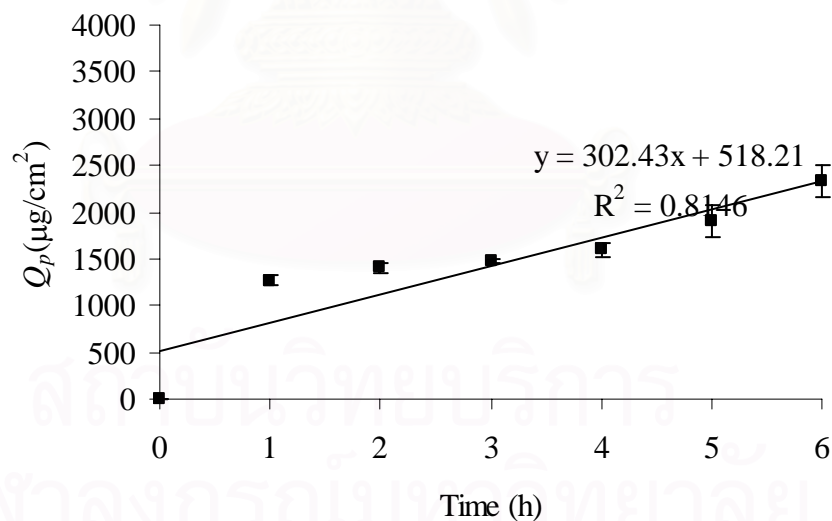


Figure 2E Permeation profiles of drug through shed snake skin (*Naja kaouthia*) for case of CS-LC-Ps (LC:CS mass ratio = 0.5:1). Q_p =Cumulative amount of permeated drug through a unit area of shed snake skin, $\mu\text{g}/\text{cm}^2$, t =time (h). Each data represents the mean \pm SD (n=3).

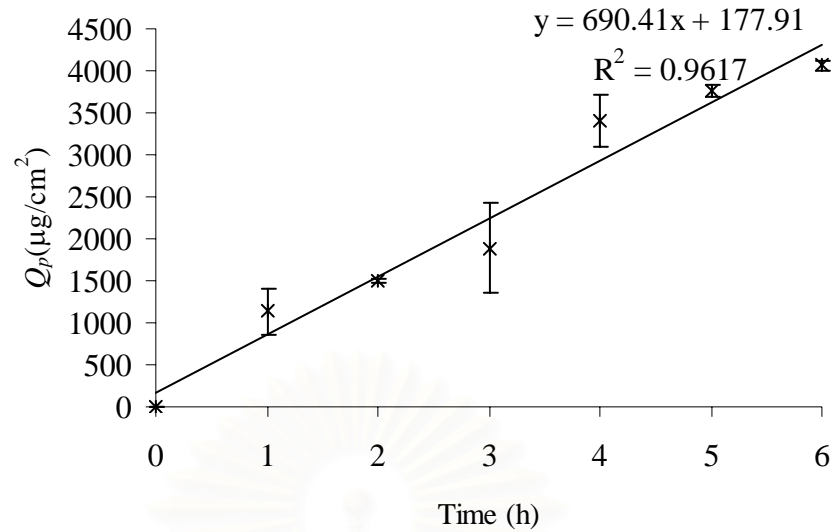


Figure 3E Permeation profiles of drug through shed snake skin (*Naja kaouthia*) for case of CS-LC-Ps (LC:CS mass ratio = 1:1). Q_p =Cumulative amount of permeated drug through a unit area of shed snake skin, $\mu\text{g}/\text{cm}^2$, t =time (h). Each data represents the mean \pm SD (n=3).

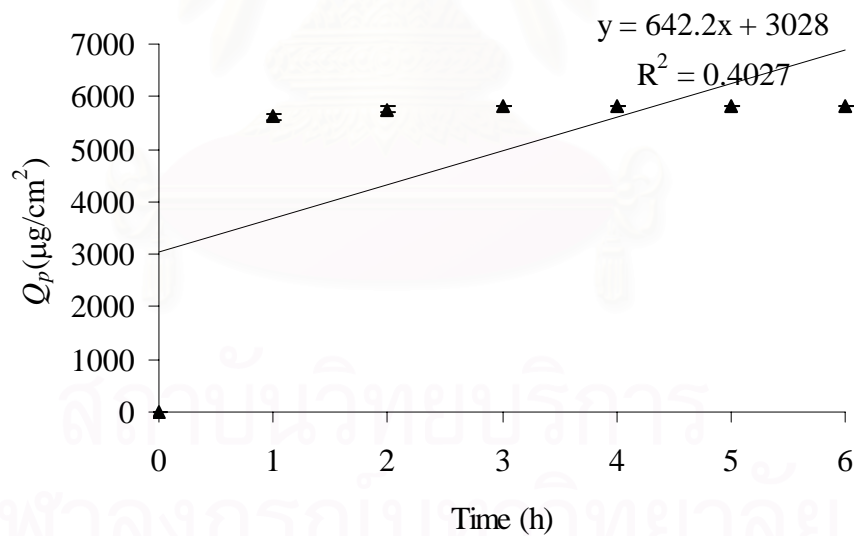


Figure 4E Permeation profiles of drug through shed snake skin (*Naja kaouthia*) for case of LC. Q_p =Cumulative amount of permeated drug through a unit area of shed snake skin, $\mu\text{g}/\text{cm}^2$, t =time (h). Each data represents the mean \pm SD (n=3).

Appendix F

In Vitro Membrane Permeation

Table 1F Cumulative amount of permeated drug through a unit area of cellulose membrane (Q_p), $\mu\text{g}/\text{cm}^2$ for case of LC:CS mass ratio = 0.33:1

Time (hour)	Q_p (1)	Q_p (2)	Q_p (3)	Mean	SD
0	0	0	0	0	0
1	486.57	491.46	523.82	500.62	20.24
2	531.1	566.96	568.58	555.55	21.19
3	631.54	641.28	763.1	678.64	73.31
4	783.36	829.72	878.2	830.43	47.42
5	886.42	1052.37	1820.96	1253.3	498.6
6	1874.53	1972.12	2171.31	2006	151.26

Table 2F Cumulative amount of permeated drug through a unit area of cellulose membrane (Q_p), $\mu\text{g}/\text{cm}^2$ for case of LC:CS mass ratio = 0.5:1

Time (hour)	Q_p (1)	Q_p (2)	Q_p (3)	Mean	SD
0	0	0	0	0	0
1	659.12	735.33	739.95	711.47	45.39
2	762.99	792.38	824.03	793.13	30.53
3	845.96	891.67	924.51	887.38	39.45
4	973.79	1071.38	1124.28	1056.5	76.34
5	1325.38	1754.88	1932.4	1670.9	312.1
6	1951.02	2133.68	2245.59	2110.1	148.7

Table 3F Cumulative amount of permeated drug through a unit area of cellulose membrane (Q_p), $\mu\text{g}/\text{cm}^2$ for case of LC:CS mass ratio = 1:1

Time (hour)	Q_p (1)	Q_p (2)	Q_p (3)	Mean	SD
0	0	0	0	0	0
1	895.58	941.23	1121.8	986.2	119.63
2	1122.56	1125.23	1160.28	1136	21.05
3	1184.82	1273.33	1278.3	1245.5	52.6
4	1314.59	1465.84	1923.23	1567.9	316.89
5	2323.51	2349.97	2544.19	2405.9	120.5
6	2546.38	2588.4	2975.51	2703.4	236.56

Table 4F Cumulative amount of permeated drug through a unit area of cellulose membrane (Q_p), $\mu\text{g}/\text{cm}^2$ for case of LC without chitosan

Time (hour)	Q_p (1)	Q_p (2)	Q_p (3)	Mean	SD
0	0	0	0	0	0
1	5342.37	5372.45	5260.16	5325	58.13
2	5346.42	5524.37	5261	5377.3	134.37
3	5429.39	5591.5	5461.25	5494	85.89
4	5700.45	5754.59	5824.88	5760	62.39
5	5791.45	5784.49	5666.18	5747.4	70.4
6	5781.28	5796.32	5780.38	5786	8.95

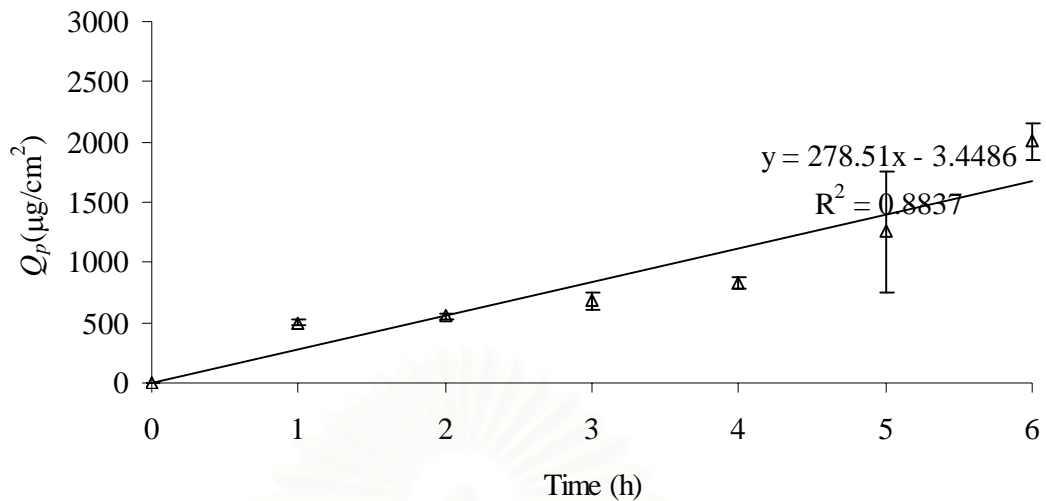


Figure 1F Permeation profiles of drug through cellulose membrane for case of CS-LC-Ps (LC:CS mass ratio = 0.33:1). Q_p =Cumulative amount of permeated drug though a unit area of shed snake skin, $\mu\text{g}/\text{cm}^2$, t =time (h). Each data represents the mean \pm SD (n=3).

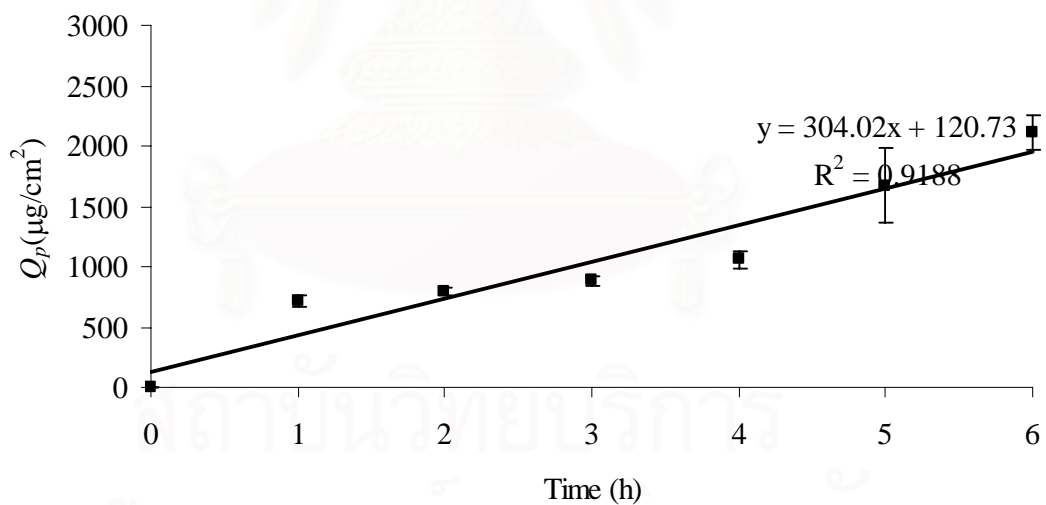


Figure 2F Permeation profiles of drug through cellulose membrane for case of CS-LC -Ps (LC:CS mass ratio = 0.5:1). Q_p =Cumulative amount of permeated drug though a unit area of shed snake skin, $\mu\text{g}/\text{cm}^2$, t =time (h). Each data represents the mean \pm SD (n=3).

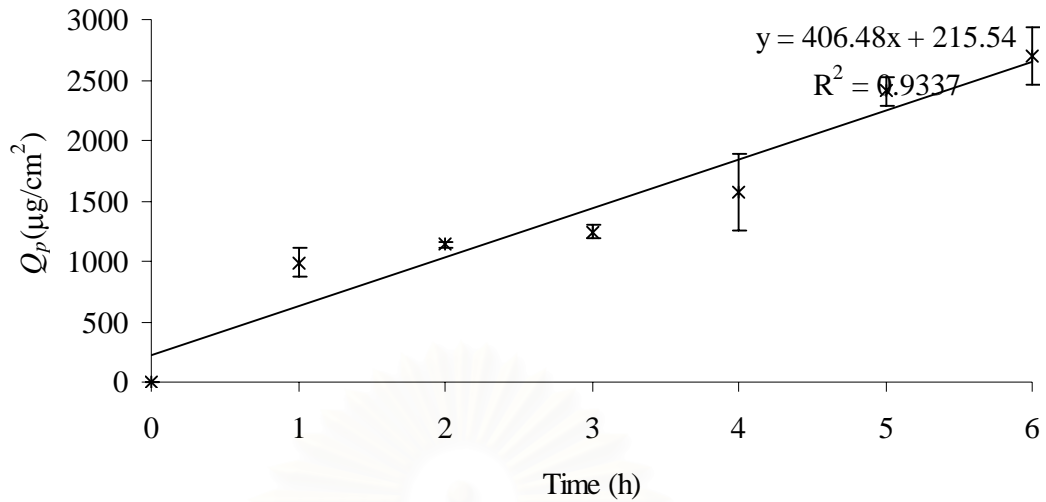


Figure 3F Permeation profiles of drug through cellulose membrane for case of CS-LC-Ps (LC:CS mass ratio = 1:1). Q_p =Cumulative amount of permeated drug through a unit area of shed snake skin, $\mu\text{g}/\text{cm}^2$, t =time (h). Each data represents the mean \pm SD (n=3).

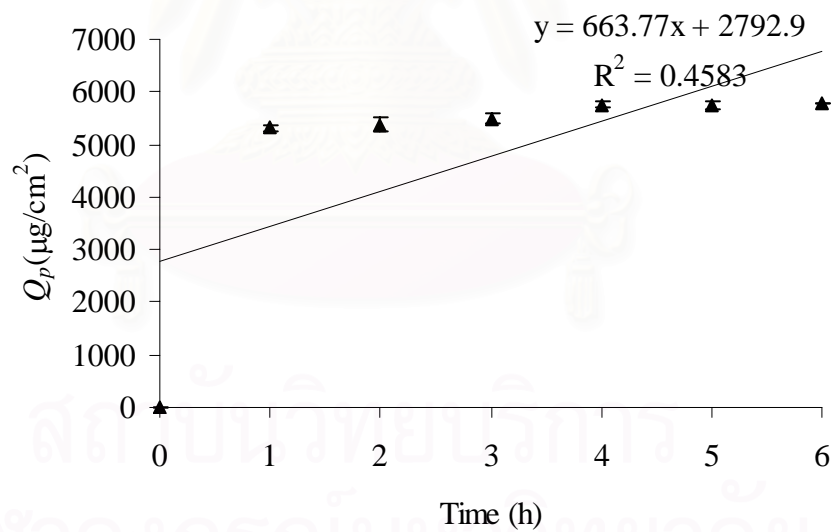


Figure 4F Permeation profiles of drug through cellulose membrane for case of LC. Q_p =Cumulative amount of permeated drug through a unit area of shed snake skin, $\mu\text{g}/\text{cm}^2$, t =time (h). Each data represents the mean \pm SD (n=3).

VITAE

Miss Wilawan Thongkong was born on February 22, 1981 in Nakhonsri Thammarat, Thailand. She graduated with a Bachelor's Degree in Chemistry from the Faculty of Education, Prince of Songkla University in 2004. She has been a graduate student in the Program of Petrochemistry and Polymer Science, Faculty of Science, Chulalongkorn University since 2005 and graduated in May 2008.

Lists of presentation:

1. May 10-11, 2007 : 1st Polymer Graduate Congress, Mahidol University
2. October 18-20, 2007 : 33rd Congress on Science and Technology of Thailand, Walailak University
3. December 12-14, 2007 : 3rd Mathematics and Physical Sciences Graduate Congress (MPSGC), Malaya University, Malaysia

สถาบันวิทยบริการ
จุฬาลงกรณ์มหาวิทยาลัย